

# NATIONAL ADVISORY COMMITTEE FOR AERONAUTICS

TECHNICAL NOTE 3605

THEORETICAL SPAN LOAD DISTRIBUTIONS  
AND ROLLING MOMENTS FOR SIDESLIPPING WINGS OF ARBITRARY  
PLAN FORM IN INCOMPRESSIBLE FLOW

By M. J. Queijo

Langley Aeronautical Laboratory  
Langley Field, Va.



Washington

December 1955

THEORETICAL SPAN LOAD DISTRIBUTIONS  
AND ROLLING MOMENTS FOR SIDESLIPPING WINGS OF ARBITRARY  
PLAN FORM IN INCOMPRESSIBLE FLOW

By M. J. Queijo

SUMMARY

A method of computing span loads and the resulting rolling moments for sideslipping wings of arbitrary plan form in incompressible flow is derived. The method requires that the span load at zero sideslip be known for the wing under consideration. Because this information is available for a variety of wings, this requirement should not seriously restrict the application of the present method. The basic method derived herein requires a mechanical differentiation and integration to obtain the rolling moment for the general wing in sideslip. For wings having straight leading and trailing edges over each semispan, the rolling moment due to sideslip is given by a simple equation in terms of plan-form parameters and the lateral center of pressure of the lift due to angle of attack.

The mechanical differentiation and integration required to obtain the rolling moment for the general wing can be avoided by use of a step-load method which is also derived. Charts are presented from which the rolling-moment parameter  $C_{l_p}/C_L$  can be obtained for wings having straight leading and trailing edges over each semispan.

Calculated span loads and rolling-moment parameters are compared with experimental values. The comparison indicates good agreement between calculations and available experimental data.

INTRODUCTION

The span load distributions and rolling moments of a wing in sideslip are important in considering the structural and dynamic lateral-stability requirements of an aircraft and, hence, have been the subject of numerous experimental and theoretical studies. Most of the studies have been limited to the determination of the rolling moment due to sideslip  $C_{l_p}$ ; however, a few studies have been concerned with the span load

distributions for wings in sideslip. (See refs. 1, 2, and 3, for example.) References 1 and 2 are theoretical studies: reference 1, for unswept wings; and reference 2, for sweptback wings. Comparisons between experimental and theoretical span loads for unswept wings showed good agreement (ref. 1). The few comparisons in reference 2 between theoretical and experimental span loads for swept wings indicated fair agreement over most of the semispan but poor agreement near the wing tip where the theory indicated a rapid decrease in load and experiments indicated a rapid increase. The method of reference 1 does predict the rapid tip-load change with sideslip which has also been observed for unswept wings. Examination of reference 1 indicated that the basic concepts employed therein could be used in the calculation of span loads and rolling moments for swept wings in sideslip, provided sweep effects could be taken into account.

The purpose of the present paper is to derive a method, using the basic concepts of reference 1 and introducing a means to account for sweep effects, which permits the calculation of the span load distribution and rolling moment for any wing in sideslip. The method requires that the span load distribution at zero sideslip angle be known. Since this information is available for a large variety of wings (see refs. 4 to 7, for example), this restriction is not believed to be serious.

The basic concepts used herein permit the determination of the span load and the resulting rolling-moment coefficient of a wing in sideslip by use of either an integration method and a continuous spanwise circulation distribution or a series summation in combination with a stepped circulation distribution. Both methods are developed herein.

### SYMBOLS

A	aspect ratio, $b^2/S$
b	span
$C_L$	wing lift coefficient due to angle of attack, $\frac{\text{Wing lift due to } \alpha}{\frac{1}{2}\rho V^2 S}$
$C_l$	wing rolling-moment coefficient, $\frac{\text{Wing rolling moment}}{\frac{1}{2}\rho V^2 S b}$
$C_{l_\beta} = \frac{\partial C_l}{\partial \beta}$	

$c$  chord, parallel to plane of symmetry

$$\frac{cc_l}{\bar{c}C_{L\beta}} = \frac{\partial^2 \gamma}{\partial \beta \partial C_L}$$

$\bar{c}$  average chord,  $S/b$

$c_i$  chord at inboard end of a vortex

$c_l$  section lift coefficient,  $\frac{\text{Section lift}}{\frac{1}{2}\rho V^2 c}$

$$c_{l_\alpha} = \frac{\partial c_l}{\partial \alpha}$$

$(c_l)_\alpha$  section lift coefficient due to angle of attack

$(c_l)_\beta$  section lift coefficient due to sideslip

$(c_l)_{\beta=0}$  section lift coefficient at zero sideslip angle

$c_o$  chord at outboard end of a vortex

$l$  section lift (lift per unit span)

$l'$  rolling moment due to one horseshoe vortex

$N$  number of horseshoe vortices representing wing

$n$  index which indicates a specific horseshoe vortex

$S$  wing area

$s$  semispan of a horseshoe vortex

$V$  free-stream velocity

$y$  spanwise distance from plane of symmetry

$\bar{y}$  spanwise position of center of pressure due to angle-of-attack load on one semispan

$z$  distance along quarter-chord line, measured from plane of symmetry

$\alpha$	geometric angle of attack, radians
$\alpha_i$	induced angle of attack, radians
$\beta$	sideslip angle, radians
$\Gamma_y$	vortex strength in spanwise direction
$(\Gamma_y)_{\beta=0}$	vortex strength $\Gamma_y$ for wing at zero sideslip angle
$\Gamma_z$	vortex strength along quarter-chord line
$\gamma$	section load parameter for total load on section, $\frac{cc_l}{\bar{c}}$
$(\gamma)_{\alpha}$	section load parameter due to angle of attack
$(\gamma)_{\beta}$	section load parameter due to sideslip
$(\gamma)_{\beta=0}$	section load parameter at zero sideslip angle
$(\gamma)_{\theta}$	section load parameter due to twist
$\theta$	local angle of attack due to twist, radians
$\kappa$	factor from reference 1
$\Lambda$	sweep of quarter-chord line, deg (positive for sweepback)
$\lambda$	taper ratio, $\frac{\text{Tip chord}}{\text{Root chord}}$
$\rho$	mass density of air

## Superscript:

- \* denotes that factor has been made nondimensional by dividing by  $b/2$ ; for example,  $c^* = \frac{c}{b/2}$

## ANALYSIS

In making span-load calculations, the wing is generally represented by a system of vortices. For the case of zero sideslip, the unswept wing can be represented by a system of spanwise and chordwise vortices as shown in figure 1(a). For wings of high aspect ratio, the spanwise vortices are generally replaced by a single vortex, and the resulting system (fig. 1(b)) is the common lifting-line-theory representation of a wing at zero sideslip angle.

Various systems of vortices have been considered for the representation of unswept wings in sideslip. One system is a modification of the lifting-line-theory representation and consists of a single spanwise vortex and a sheet of trailing vortices which are parallel to the free airstream (fig. 1(c)). This system was used by Blenk (ref. 8); however, his calculated rolling moments due to sideslip were opposite in sign from those obtained experimentally.

The vortex system used by Weissinger for the unswept wing in sideslip is shown in figure 1(d), and this system is also a modification of the lifting-line-theory representation at zero sideslip. The theoretical arguments for the system are given in reference 1 and, therefore, will not be repeated here. However, it should be noted that the span load distributions and values of  $C_{l\beta}$  computed by Weissinger for unswept wings are generally in very good agreement with experiment.

As stated in the introduction, the basic concepts used herein are the same as those of reference 1 and are applied directly to the swept wing. The swept wing in sideslip is represented by a system of vortices, as indicated in figure 2(a), which consists of a vortex located along the wing quarter-chord line and a sheet of vortices emanating from this vortex. The vortices of the sheet are parallel to the wing plane of symmetry from the quarter-chord line to the trailing edge, and then they slant so as to be parallel to the relative wind direction. In the present paper, the portion of the vortex sheet parallel to the plane of symmetry is referred to as being made up of chordwise-bound vortices, whereas the rest of the vortex sheet is considered to be made up of trailing-free vortices.

The lift produced by a unit length of vortex is given by the Kutta-Joukowski equation

$$l = \rho V_p \Gamma$$

where  $\Gamma$  is the vortex strength (or circulation) and  $V_p$  is the velocity component perpendicular to the vortex. As may be seen from figure 2(a),

the free-stream velocity has components perpendicular to the quarter-chord-line vortex and the chordwise-bound vortices and, hence, these vortices will produce lift in accordance with the Kutta-Joukowski equation. The trailing-free vortices are parallel to the relative wind and hence produce no lift. The strength of the chordwise-bound vortices is determined by the strength distribution of the quarter-chord-line vortex; therefore, the lift distribution of the wing in sideslip can be determined, provided the distribution of the strength of the quarter-chord-line vortex for the wing in sideslip is known.

The vortex strength would be made up of the circulation due to the basic-type loading (camber and/or twist), angle-of-attack loading, and some modification to the sum of these loadings as a result of sideslip. In general, the circulation at zero sideslip can be obtained from published reports (refs. 4, 5, and 6, for example), and the remaining unknown is the modification due to sideslip. An approximate method of evaluating this effect is as follows: with reference to figure 2(b), which pertains to the right, or leading wing semispan, the lift per unit length of the quarter-chord-line vortex of a swept wing in sideslip is given by

$$l_1 = \rho V \cos(\Lambda - \beta) \Gamma_z$$

and also by

$$l_1 = \frac{1}{2} \rho V^2 \cos^2(\Lambda - \beta) c_{l_\alpha} \frac{\alpha - \alpha_i}{\cos(\Lambda - \beta)} c$$

so that the circulation  $\Gamma_z$  is

$$\Gamma_z = \frac{1}{2} V c c_{l_\alpha} (\alpha - \alpha_i)$$

Similarly, for the wing at zero sideslip, the circulation is given by

$$(\Gamma_z)_{\beta=0} = \frac{1}{2} V c c_{l_\alpha} (\alpha - \alpha_i)_{\beta=0}$$

Thus the circulation at a sideslip angle is related to the circulation at zero sideslip by

$$\Gamma_z = (\Gamma_z)_{\beta=0} \frac{\alpha - \alpha_i}{(\alpha - \alpha_i)_{\beta=0}}$$

It appears, therefore, that the local circulation of the quarter-chord-line vortex of a wing at a given angle of attack will be changed by sideslip only if sideslip changes the induced angle of attack. For infinite aspect ratio, the induced angle of attack is zero and, hence,  $\Gamma_z$  is exactly equal to  $(\Gamma_z)_{\beta=0}$ . For large aspect ratios, when  $\alpha_i$  is small relative to  $\alpha$ , a modification to  $\alpha_i$  due to sideslip probably will have a negligible effect on the local circulation. Even for small aspect ratios, when  $\alpha_i$  can be large relative to  $\alpha$ , it does not appear that a small sideslip angle should affect  $\alpha_i$  enough to change the local circulation appreciably. This argument is substantiated to some extent by calculations of the circulation distribution of unswept wings in sideslip made by Weissinger (ref. 1). These results showed that for unswept wings the change in circulation due to sideslip was small and resulted in an increment in  $C_{l\beta}/C_l$  that was independent (for practical purposes) of aspect ratio and taper ratio for a fairly wide range of both parameters.

Because of the effort involved in actually computing the circulation distribution for wings in sideslip and because of the arguments given in the preceding paragraph, the analysis of the present paper is based on the assumption that the circulation distribution for the wing in sideslip is the same as for the wing at zero sideslip. Span load distributions for the wing in sideslip can then be obtained by the methods derived in the appendix. The rolling moment due to sideslip can be obtained for any wing by integration of the span load due to sideslip, and this method is referred to herein as the integration method. For the most general case, the integration involved in this method cannot be made conveniently. In such instances a second method, wherein the wing is represented by a number of horseshoe vortices (see figs. 3 and 4), can be used. This method also is derived herein. The resulting values of the rolling-moment parameter  $C_{l\beta}$  are obtained and a small correction to account for effects of sideslip on the circulation distribution (as determined in ref. 1 for unswept wings) is applied. Although this final correction may not be strictly applicable to swept wings, it is a small quantity and should be of the right order of magnitude even for swept wings.

## RESULTS AND DISCUSSION

### General Remarks

The general equations derived in the appendix can be used to obtain span loads and rolling moments for sideslipping wings of arbitrary plan form and twist in incompressible flow. The general equations have been



used to determine equations which apply specifically to wings having straight leading and trailing edges and for wings of elliptic plan form. Equations for specific types of wings not treated herein (for example, M, W, or cranked wings) can be obtained from the general equations with little difficulty. The span loads and rolling moments for wings in sideslip can be obtained by the methods presented herein, however, only if the span load at zero sideslip angle is known. This is not a serious restriction since such information is available for a large variety of wings. However, wings of odd plan form present an additional problem in that it will generally be necessary to compute the span load at zero sideslip before proceeding to the sideslip case. In such instances, the span load at zero sideslip can be computed by using a method such as that of references 7, 9, and 10.

In the following sections, some of the equations derived in the appendix are repeated and results obtained are discussed.

#### Span Load Distribution in Sideslip

The span load distribution of a wing in sideslip can be determined from the following general equation:

$$\gamma = (\gamma)_{\beta=0}(1 \pm \beta \tan \Lambda) - \frac{3}{4} \beta c^* \frac{d(\gamma)_{\beta=0}}{dy^*} \quad (1)$$

The load due to sideslip is given by

$$(\gamma)_{\beta} = (\gamma)_{\beta=0}(\pm \beta \tan \Lambda) - \frac{3}{4} \beta c^* \frac{d(\gamma)_{\beta=0}}{dy^*} \quad (2)$$

Wherever a choice of signs is indicated, a plus sign applies to the right or leading wing semispan, and a minus sign applies to the left or trailing wing semispan.

A study of equation (2) shows that, if a portion of the total wing load is symmetric over the wing span at zero sideslip, the change in that portion of the load due to sideslip will be antisymmetric (and, hence, will produce a resultant rolling moment). On the other hand, if a portion of the total wing load is antisymmetric over the wing span at zero sideslip, the change in that portion of the load due to sideslip is symmetric (and, hence, will produce no resultant rolling moment).

In order to illustrate the effects of sideslip on span loads, the parameter  $\frac{cc_l}{cc_{l\beta}}$  has been computed for several rigid wings of aspect

ratio 4.5. This parameter can be obtained readily by expanding equation (2); thus,

$$(\gamma)_{\beta} = \left[ (\gamma)_{\theta} + \left( \frac{\gamma}{C_L} \right)_{\alpha} C_L \right] (\pm \beta \tan \Lambda) - \frac{3}{4} \beta c^* \left[ \frac{d(\gamma)_{\theta}}{dy^*} + C_L \frac{d \left( \frac{\gamma}{C_L} \right)_{\alpha}}{dy^*} \right]$$

Inasmuch as the term  $(\gamma)_{\theta}$  is independent of  $C_L$  due to angle of attack for rigid wings, differentiating with respect to  $\beta$  and  $C_L$  yields the desired parameter

$$\frac{cc_l}{\bar{c}C_L\beta} = \left( \frac{cc_l}{\bar{c}C_L} \right)_{\alpha} (\pm \tan \Lambda) - \frac{3}{4} c^* \frac{d \left( \frac{cc_l}{\bar{c}C_L} \right)_{\alpha}}{dy^*} \quad (3)$$

For elliptic wings, equation (3) reduces to

$$\frac{cc_l}{\bar{c}C_L\beta} = \pm \frac{32}{\pi^2 A} y^* \quad (4)$$

Computed values of  $\frac{cc_l}{\bar{c}C_L\beta}$  are shown in figure 5 for several wings. The

span load due to sideslip is, of course, antisymmetric and, hence, results are presented only for the right semispan. In each case the contributions of the quarter-chord-line vortex and chordwise-bound vortices are presented individually and are also combined. The results show that, for the true elliptic wing (unswept midchord line), the chordwise-bound vortices account for three-quarters of the local load coefficient and the local load coefficient varies linearly with spanwise position.

The results for the unswept wing are in qualitative agreement with the results given for unswept wings in reference 1 and indicate an infinite load coefficient at the wing tips. The effects of sweep can be seen by comparing figures 5(b) and 5(c). The local load due to sideslip associated with the quarter-chord-line vortex is, of course, a consequence of sweep and can contribute greatly to the load in sideslip.

Some comparisons between calculated and experimental span loads due to sideslip are shown in figure 6 for an untapered  $45^\circ$  sweptback wing of aspect ratio 5.16. The loads due to sideslip were computed from equation (2) and experimental values of  $(\gamma)_{\beta=0}$ . In general, the computed and experimental span loads due to sideslip are in very good agreement at low angles of attack.

## Rolling Moment Due to Sideslip

Integration method.— A general equation for the rolling moment due to sideslip is given in the appendix as

$$C_{l_\beta} = -\frac{1}{4} \left\{ \int_{-1}^0 \left[ (\gamma)_\theta \tan \Lambda + \frac{3}{4} c^* \frac{d(\gamma)_\theta}{dy^*} \right] y^* dy^* + \int_0^1 \left[ (\gamma)_\theta \tan \Lambda - \frac{3}{4} c^* \frac{d(\gamma)_\theta}{dy^*} \right] y^* dy^* \right\} - \frac{1}{2} \int_0^1 \left[ (\gamma)_\alpha \tan \Lambda - \frac{3}{4} c^* \frac{d(\gamma)_\alpha}{dy^*} \right] y^* dy^* + 0.05 C_L \quad (5)$$

If the wing under consideration has symmetrical twist, equation (5) can be written as

$$C_{l_\beta} = -\frac{1}{2} \int_0^1 \left\{ \left[ (\gamma)_\theta + (\gamma)_\alpha \right] \tan \Lambda - \frac{3}{4} c^* \left[ \frac{d(\gamma)_\theta}{dy^*} + \frac{d(\gamma)_\alpha}{dy^*} \right] \right\} y^* dy^* + 0.05 C_L \quad (6)$$

The rate of change of  $C_{l_\beta}$  with  $C_L$  for rigid wings is given by

$$\frac{C_{l_\beta}}{C_L} = -\frac{1}{2} \bar{y}^* \tan \Lambda + \frac{3}{8} \int_0^1 c^* \frac{d\left(\frac{\gamma}{C_L}\right)_\alpha}{dy^*} y^* dy^* + 0.05 \quad (7)$$

which, for wings having straight leading and trailing edges over each semispan, reduces to

$$\frac{C_{l_\beta}}{C_L} = -\frac{1}{2} \left\{ \frac{3}{A(1+\lambda)} + \bar{y}^* \left[ \tan \Lambda + \frac{6(1-\lambda)}{A(1+\lambda)} \right] \right\} + 0.05 \quad (8)$$

For elliptic wings (having unswept midchord lines), the parameter  $C_{l_\beta}/C_L$  is given by

$$\frac{C_{l_\beta}}{C_L} = -\frac{16}{3\pi^2 A} + 0.05 \quad (9)$$

Equation (8) has been used to evaluate the parameter  $C_{l\beta}/C_L$  for rigid wings covering a wide range of aspect ratio, taper ratio, and sweep, and having straight leading and trailing edges over each semispan. The values of  $\bar{y}^*$  used in equation (8) were obtained from references 4, 5, and 6. The results are given in figure 7.

Some comparisons of values of  $C_{l\beta}/C_L$  computed from the equations presented herein with those of other theories are shown in figures 8, 9, and 10. The variation of  $C_{l\beta}/C_L$  with aspect ratio for elliptic wings was computed by using equation (9) and is shown in figure 8. The computed values are somewhat greater than those given in equation (4) of reference 1 with  $\kappa = 1.5$ . The primary reason for the difference in the curves is that the effects of the quarter-chord-line vortex were not considered in reference 1. Omission of these effects in the present analysis yields a curve of  $C_{l\beta}/C_L$  against aspect ratio which is in close agreement with Weissinger's curve. The remaining difference between the two curves (when the quarter-chord-line vortex is neglected) is present because, for elliptic wings, reference 1 evaluated the increment in  $C_{l\beta}/C_L$  due to the small change in vortex strength associated with side-slip by an exact expression which is slightly different from the value of 0.05 used herein.

Values of  $C_{l\beta}/C_L$  computed from equation (8) are compared in figure 9 with those from reference 1 for unswept wings having straight leading and trailing edges. In reference 1, Weissinger derives the following equation for this type of wing:

$$\frac{C_{l\beta}}{C_L} = - \frac{\kappa}{A} \frac{0.71\lambda + 0.29}{-1 + \lambda} + 0.05 \quad (10)$$

The reference also states that the exact theory fixes the value of  $\kappa$  at 1.5, but that, from comparison with experiment, a more practical value is  $\kappa = 1.0$ . The practice in the past therefore has been to use this equation with  $\kappa = 1.0$  for unswept wings; and, in instances where sweep has been considered, the same equation generally has been used and an increment due to sweep then added. (See ref. 11, for example.) Tests of present-day wings generally have shown more negative values of  $C_{l\beta}/C_L$  than those predicted by equation (10) with  $\kappa = 1.0$ , but these values are in good agreement with calculated values if  $\kappa = 1.5$  is used. It appears likely that the value of  $\kappa$  considered practical by Weissinger was based on tests of wings which were in use at the time the investigation was made. These wings generally had rounded tips, which would tend to reduce the tip loading and, hence, also reduce  $C_{l\beta}/C_L$ .

Figure 9 presents a comparison of values of  $C_{l_\beta}/C_L$  from figure 7 (computed from eq. (8)) with theoretical values from reference 1 (computed from eq. (10)). Agreement between the values is good when  $\kappa = 1.5$  is used in equation (10); in fact, with  $\kappa = 1.5$ , equations (8) and (10) are identical for a taper ratio of 1.0 and zero sweep.

Values of  $C_{l_\beta}/C_L$  computed from equation (8) for untapered  $45^\circ$  swept-back wings are compared in figure 10 with values from reference 11. The values from reference 11 are somewhat lower than those of the present paper. Most of the difference is associated with the fact that the values of reference 11 are in part made up of the value for unswept wings determined by Weissinger's equation, equation (10), with  $\kappa = 1.0$ . The remaining difference is associated with the contribution to  $C_{l_\beta}$  due to sweep. A comparison of equation (17) of reference 11 and equation (8) of the present paper shows that the remaining difference is due to an induction factor  $\frac{A + 2 \cos \Lambda}{A + 4 \cos \Lambda}$  used in reference 11 to account for induced effects because of the antisymmetric load due to sideslip. No such induction factor appears in the present paper because it has been argued that the circulation remains symmetric even when the wing is sideslipping.

Some comparisons of experimental and calculated low-speed values of  $C_{l_\beta}/C_L$  are shown in figures 11 and 12. The present theory correctly predicts effects of sweep, aspect ratio, and taper ratio, and the calculated values also generally agree quantitatively with experimental data from references 12 to 15.

Step-load method.—As stated previously, the advantage of using the step-load method instead of the integration method is that any integration or differentiation is avoided and, hence, the method is convenient to use for wings having the following characteristics: (1) chords which are not simple functions of spanwise position and (2) loads which are associated with twist.

The general equation for the rolling moment is derived in the appendix and is

$$C_l = -\frac{1}{2N^2} \sum_{n=-N/2}^{n=-1} \left\{ (2n+1)(1 - \beta \tan \Lambda) - \frac{3}{4} \beta N [nc_o^* - (n+1)c_i^*] \right\} [\gamma]_{\beta=0} n -$$

$$\frac{1}{2N^2} \sum_{n=1}^{n=N/2} \left\{ (2n-1)(1 + \beta \tan \Lambda) + \frac{3}{4} \beta N [nc_o^* - (n-1)c_i^*] \right\} [\gamma]_{\beta=0} n + 0.05\beta C_L \quad (11)$$

If the wing is symmetric, the rolling moment due to sideslip is

$$C_{l\beta} = - \frac{1}{N^2} \sum_{n=1}^{n=N/2} \left\{ (2n - 1) \tan \Lambda + \right. \\ \left. \frac{3}{4} N \left[ nc_o^* - (n - 1)c_i^* \right] \right\} \left[ (\gamma)_{\beta=0} \right]_n + 0.05 C_L \quad (12)$$

If in addition to being symmetric, the wing is also rigid, then the rate of change of  $C_{l\beta}$  with  $C_L$  is given by

$$\frac{C_{l\beta}}{C_L} = - \frac{1}{N^2} \sum_{n=1}^{n=N/2} \left\{ (2n - 1) \tan \Lambda + \right. \\ \left. \frac{3}{4} N \left[ nc_o^* - (n - 1)c_i^* \right] \right\} \left[ \left( \frac{\gamma}{C_L} \right)_{\alpha} \right]_n + 0.05 \quad (13)$$

In order to determine the compatibility of the integration and step-load methods, values of  $C_{l\beta}/C_L$  for several rigid, symmetrical wings were computed and the results are presented in figure 13. The results show that values of  $C_{l\beta}/C_L$  computed by the step-load method converge rapidly on the values from the integration method as the number of horseshoe vortices used in the step-load method is increased. About 20 horseshoe vortices should be sufficient for a reasonable representation of a wing.

Equation (12) was used to compute the increment in  $C_{l\beta}$  due to linear twist for a wing having an aspect ratio of 4.0, a taper ratio of 0.6,  $45^\circ$  sweep of the leading edge, and  $-6^\circ$  maximum twist at the wing tips. Values of  $(\gamma)_\theta$  used in the calculations were obtained by interpolation of the material in reference 6. The computed value of  $C_{l\beta}$  due to twist at  $\alpha = 0^\circ$  was 0.05, a value which compares well with the experimental value of 0.04 (ref. 16).

## CONCLUDING REMARKS

A method of computing span loads and the resulting rolling moments for sideslipping wings of arbitrary plan form in incompressible flow is derived. The method requires that the span load at zero sideslip be known for the wing under consideration. Since this information is available for a large variety of wings, this requirement should not seriously restrict the application of the present method. The basic method derived herein requires a mechanical differentiation and integration to obtain the rolling moment for the general wing in sideslip. For wings having straight leading and trailing edges over each semispan, the rolling moment due to sideslip is given by a simple equation in terms of the plan-form parameters and the lateral center of pressure of the lift due to angle of attack.

The mechanical differentiation and integration required to obtain the rolling moment for the general wing can be avoided by a step-load method which is also derived herein.

Charts are presented from which the rolling-moment parameter  $C_{l_p}/C_L$  can be obtained for wings having straight leading and trailing edges over each semispan.

Calculated span loads and rolling-moment parameters are compared with experimental values. The comparison indicates good agreement between calculations and available experimental data.

Langley Aeronautical Laboratory,  
National Advisory Committee for Aeronautics,  
Langley Field, Va., October 6, 1955.

## APPENDIX

## DERIVATION OF EQUATIONS

## General Equations From Integration Method

In the following derivation, all equations refer to the right or leading wing semispan unless otherwise noted. The considerations presented in the section entitled "Analysis" permit lift to be obtained from the quarter-chord-line vortex and from the chordwise-bound vortices. By referring to figure 2(b), it is seen that, for the right (leading) wing semispan, the lift per unit length of the quarter-chord-line vortex of a swept wing in sideslip is given by

$$l_1 = \rho V \cos(\Lambda - \beta) \Gamma_z$$

or, per unit length of wing span, by

$$l_1 = \rho V \cos(\Lambda - \beta) \Gamma_z \frac{1}{\cos \Lambda}$$

The lift due to one chordwise-bound vortex is

$$l_2 = - \rho V \sin \beta \left( \frac{3}{4} c \right) \frac{d\Gamma_z}{dz}$$

For small sideslip angles such that  $\sin \beta = \beta$  and  $\cos \beta = 1.0$ , the lift component per unit of wing span for the quarter-chord-line vortex is

$$l_1 = \rho V \Gamma_z (1 + \beta \tan \Lambda) \quad (A1)$$

and for the chordwise-bound vortex,

$$l_2 = - \frac{3}{4} \rho V c \beta \frac{d\Gamma_z}{dz} \quad (A2)$$

In general, span load or circulation distributions are presented in terms of the spanwise circulation strength  $\Gamma_y$  rather than the strength  $\Gamma_z$  along the quarter-chord line. The relationship between  $\Gamma_y$  and  $\Gamma_z$  can be determined readily from consideration of the lift on a wing at



zero sideslip angle. The lift per unit span is given by

$$(l)_{\beta=0} = \rho V \Gamma_y \quad (A3)$$

and also by

$$(l)_{\beta=0} = \rho V \Gamma_z \cos \Lambda \frac{1}{\cos \Lambda}$$

from which it is seen that  $\Gamma_y$  and  $\Gamma_z$  are equal. Equations (A1) and (A2) therefore can be written as:

$$l_1 = \rho V \Gamma_y (1 + \beta \tan \Lambda) \quad (A4)$$

and

$$l_2 = - \frac{3}{4} \rho V c \beta \frac{d\Gamma_y}{dy} \quad (A5)$$

The vortex strength  $\Gamma_y$  is related to the section lift at zero sideslip by equation (A3) or, in coefficient form, by

$$\Gamma_y = \frac{1}{2} V c (c_l)_{\beta=0} \quad (A6)$$

Substituting equation (A6) into equations (A4) and (A5), adding the resulting equations, and nondimensionalizing yields the following general equation for determining the span load distribution:

$$\gamma = (\gamma)_{\beta=0} (1 + \beta \tan \Lambda) - \frac{3}{4} \beta c^* \frac{d(\gamma)_{\beta=0}}{dy^*} \quad (A7)$$

Similarly, for the left (or trailing) wing semispan, it can be shown that

$$\gamma = (\gamma)_{\beta=0} (1 - \beta \tan \Lambda) - \frac{3}{4} \beta c^* \frac{d(\gamma)_{\beta=0}}{dy^*} \quad (A8)$$

Equations (A7) and (A8) can be used to determine the span load on a wing in sideslip, provided that the load at zero sideslip is known. The load due to sideslip for the right semispan is

$$(\gamma)_{\beta} = (\gamma)_{\beta=0} \beta \tan \Lambda - \frac{3}{4} \beta c^* \frac{d(\gamma)_{\beta=0}}{dy^*} \quad (A9)$$

and for the left semispan,

$$(\gamma)_{\beta} = -(\gamma)_{\beta=0} \beta \tan \Lambda - \frac{3}{4} \beta c^* \frac{d(\gamma)_{\beta=0}}{dy^*} \quad (A10)$$

The parameter  $(\gamma)_{\beta=0}$  is made up of the components  $(\gamma)_{\theta}$  and  $(\gamma)_{\alpha}$ . For rigid wings, only  $(\gamma)_{\alpha}$  varies with  $C_L$ , and, therefore, the rate of change of load due to sideslip with  $C_L$  is given by the following equation for the right wing semispan:

$$\frac{\partial(\gamma)_{\beta}}{\partial C_L} = \left(\frac{\gamma}{C_L}\right)_{\alpha} \beta \tan \Lambda - \frac{3}{4} \beta c^* \frac{d\left(\frac{\gamma}{C_L}\right)_{\alpha}}{dy^*}$$

A second differentiation, with respect to  $\beta$ , yields the following load parameters:

For the right semispan,

$$\frac{cc_l}{\bar{c}C_L\beta} = \left(\frac{cc_l}{\bar{c}C_L}\right)_{\alpha} \tan \Lambda - \frac{3}{4} c^* \frac{d\left(\frac{cc_l}{\bar{c}C_L}\right)_{\alpha}}{dy^*} \quad (A11)$$

For the left semispan,

$$\frac{cc_l}{\bar{c}C_L\beta} = -\left(\frac{cc_l}{\bar{c}C_L}\right)_{\alpha} \tan \Lambda - \frac{3}{4} c^* \frac{d\left(\frac{cc_l}{\bar{c}C_L}\right)_{\alpha}}{dy^*} \quad (A12)$$

The rolling moment of a wing in sideslip can be determined by an integration of the span load multiplied by the proper moment arm. A general form of a rolling-moment equation is obtained from equations (A7) and (A8), to which must be added the increment determined by Weissinger (ref. 1) for unswept wings and which is supposed to account for the small modification in circulation strength  $\Gamma_y$  due to sideslip. Thus, the rolling-moment equation is

$$C_l = \frac{1}{4} \left[ \int_{-1}^0 \gamma y^* dy^* - \int_0^1 \gamma y^* dy^* \right] + 0.05 \beta C_L \quad (A13)$$

where  $\gamma$  for the left wing semispan is used in the first integral and  $\gamma$  for the right wing semispan is used in the second integral. The rolling moment due to sideslip is determined by substituting equations (A7) and (A8) into equation (A13) and differentiating with respect to  $\beta$ . The result can be shown to be, in expanded form,

$$C_{l\beta} = -\frac{1}{4} \left\{ \int_{-1}^0 \left[ (\gamma)_{\theta} \tan \Lambda + \frac{3}{4} c^* \frac{d(\gamma)_{\theta}}{dy^*} \right] y^* dy^* + \int_0^1 \left[ (\gamma)_{\theta} \tan \Lambda - \frac{3}{4} c^* \frac{d(\gamma)_{\theta}}{dy^*} \right] y^* dy^* \right\} - \frac{1}{2} \int_0^1 \left[ (\gamma)_{\alpha} \tan \Lambda - \frac{3}{4} c^* \frac{d(\gamma)_{\alpha}}{dy^*} \right] y^* dy^* + 0.05 C_L \quad (A14)$$

The rate of change of  $C_{l\beta}$  with  $C_L$  for a rigid wing is given by

$$\frac{C_{l\beta}}{C_L} = -\frac{1}{2} \int_0^1 \left[ \left( \frac{\gamma}{C_L} \right)_{\alpha} \tan \Lambda - \frac{3}{4} c^* \frac{d \left( \frac{\gamma}{C_L} \right)_{\alpha}}{dy^*} \right] y^* dy^* + 0.05 \quad (A15)$$

Equation (A15) can be reduced by noting that the first term on the right-hand side can be integrated by inspection; that is,

$$\int_0^1 \left( \frac{\gamma}{C_L} \right)_{\alpha} \tan \Lambda y^* dy^* = \bar{y}^* \tan \Lambda \quad (A16)$$

The second term of equation (A15) can be simplified by integration by parts, so that equation (A15) becomes

$$\frac{C_{l\beta}}{C_L} = -\frac{1}{2} \bar{y}^* \tan \Lambda - \frac{3}{8} \int_0^1 \left( \frac{\gamma}{C_L} \right)_{\alpha} \left( c^* + y^* \frac{dc^*}{dy^*} \right) dy^* + 0.05 \quad (A17)$$

Equation (A17) can, of course, be further simplified if  $c^*$  is a simple function of spanwise position.

The differentiation and integration indicated in the various rolling-moment equations can be avoided by use of the step-load method which is developed in the following section.

## General Equations From Step-Load Method

The basic assumptions of the step-load method of determining the span load and rolling moment of a wing in sideslip are identical to those of the integration method. In the step-load method the span load distribution at zero sideslip angle is approximated by a number  $N$  of equal-span horseshoe vortices which are oriented and numbered as shown in figures 3 and 4. By considering one horseshoe vortex with its center at spanwise position  $y_n$  (see fig. 4 for details), it is readily seen that lift is produced by the quarter-chord-line-vortex segment and the two chordwise-bound vortices of the horseshoe vortex. The lift due to one horseshoe vortex on the right wing semispan is

$$\text{Lift} = \rho V \cos(\Lambda - \beta) \Gamma_y \frac{2s}{\cos \Lambda} + \rho V \sin \beta \Gamma_y \left( \frac{3}{4} c_o - \frac{3}{4} c_i \right)$$

or, when small sideslip angles are assumed,

$$\text{Lift} = 2spV\Gamma_y(1 + \beta \tan \Lambda) + \frac{3}{4} \rho V \Gamma_y \beta (c_o - c_i) \quad (\text{A18})$$

The step-load method results in a total load on each horseshoe vortex made up of a distributed load due to the quarter-chord-line-vortex segment and two concentrated loads (concentrated relative to spanwise position) due to the chordwise-bound vortices. It appears, therefore, that the step-load method does not lend itself to the determination of a continuous span load distribution.

The loads given by equation (A18) can, of course, be used to determine the rolling moment of the wing. The rolling moment due to each horseshoe vortex is obtained by multiplying the load on each lift-producing element by its moment arm; therefore,

$$l' = -2spV\Gamma_y(1 + \beta \tan \Lambda) - \frac{3}{4} \rho V \Gamma_y \beta [(y + s)c_o - (y - s)c_i]$$

This equation can be simplified to

$$l' = -\rho V \Gamma_y \left\{ 2s(1 + \beta \tan \Lambda) + \frac{3}{4} \beta \left[ \left(1 + \frac{s}{y}\right)c_o - \left(1 - \frac{s}{y}\right)c_i \right] \right\} \quad (\text{A19})$$

Substitution of equation (A6) into equation (A19) yields

$$l' = -\frac{1}{2} \rho V^2 \gamma c_l \beta \left\{ 2s(1 + \beta \tan \Lambda) + \frac{3}{4} \beta \left[ \left(1 + \frac{s}{y}\right)c_o - \left(1 - \frac{s}{y}\right)c_i \right] \right\} \quad (\text{A20})$$

The spanwise distance to the center of a horseshoe vortex on the right wing semispan is given by

$$y = (2n - 1)s$$

Therefore, equation (A20) can be written as

$$l' = -\frac{1}{2} \rho V^2 c (c_l)_{\beta=0} (2n - 1)s \left\{ 2s(1 + \beta \tan \Lambda) + \frac{3}{4} \beta \left[ \left(1 + \frac{1}{2n - 1}\right) c_o - \left(1 - \frac{1}{2n - 1}\right) c_i \right] \right\}$$

This equation can be simplified further by algebraic manipulation to obtain

$$l' = -\rho V^2 c (c_l)_{\beta=0} s^2 \left\{ (2n - 1)(1 + \beta \tan \Lambda) + \frac{3}{4} \beta \left[ \frac{nc_o}{s} - (n - 1) \frac{c_i}{s} \right] \right\}$$

Similarly it can be shown that, for the left or trailing wing semispan, the rolling moment due to one vortex is given by

$$l' = -\rho V^2 c (c_l)_{\beta=0} s^2 \left\{ (2n + 1)(1 - \beta \tan \Lambda) - \frac{3}{4} \beta \left[ \frac{nc_o}{s} - (n + 1) \frac{c_i}{s} \right] \right\}$$

The horseshoe-vortex semispan is related to the wing span by  $b = 2Ns$ ; hence, the rolling moment per vortex on the right wing semispan can be written as

$$l' = -\rho V^2 c (c_l)_{\beta=0} \frac{b^2}{4N^2} \left\{ (2n - 1)(1 + \beta \tan \Lambda) + \frac{3}{4} \beta N \left[ nc_o^* - (n - 1)c_i^* \right] \right\} \quad (A21)$$

and on the left wing semispan as

$$l' = -\rho V^2 c (c_l)_{\beta=0} \frac{b^2}{4N^2} \left\{ (2n + 1)(1 - \beta \tan \Lambda) - \frac{3}{4} \beta N \left[ nc_o^* - (n + 1)c_i^* \right] \right\} \quad (A22)$$

The most general form for the rolling-moment coefficient is obtained by summing equations (A21) and (A22) over the wing span and adding the correction determined by Weissinger in reference 1. The result is

$$C_l = - \frac{1}{2N^2} \sum_{n=-N/2}^{n=-1} \left\{ (2n+1)(1-\beta \tan \Lambda) - \frac{3}{4} \beta N [nc_o^* - (n+1)c_i^*] \right\} [\gamma]_{\beta=0}_n - \frac{1}{2N^2} \sum_{n=1}^{n=N/2} \left\{ (2n-1)(1+\beta \tan \Lambda) + \frac{3}{4} \beta N [nc_o^* - (n-1)c_i^*] \right\} [\gamma]_{\beta=0}_n + 0.05\beta C_L \quad (A23)$$

If the wing is symmetrical, then it is necessary only to integrate over one semispan, multiply the result by two, and add the  $0.05\beta C_L$  increment. The rolling moment due to sideslip for a symmetrical wing is given by

$$C_{l_\beta} = - \frac{1}{N^2} \sum_{n=1}^{n=N/2} \left\{ (2n-1)\tan \Lambda + \frac{3}{4} N [nc_o^* - (n-1)c_i^*] \right\} [\gamma]_{\beta=0}_n + 0.05C_L \quad (A24)$$

For rigid wings, the rate of change of  $C_{l_\beta}$  with  $C_L$  is given by

$$\frac{C_{l_\beta}}{C_L} = - \frac{1}{N^2} \sum_{n=1}^{n=N/2} \left\{ (2n-1)\tan \Lambda + \frac{3}{4} N [nc_o^* - (n-1)c_i^*] \right\} \left[ \left( \frac{\gamma}{C_L} \right)_\alpha \right]_n + 0.05 \quad (A25)$$

The various equations can be simplified if  $c_o$  and  $c_i$  are simple functions of spanwise position.

#### Equations for Specific Types of Wings

Elliptic wings - integration method.- Elliptic wings have geometric and aerodynamic load characteristics at zero sideslip which can be

defined by simple mathematical expressions; hence, some of their aerodynamic derivatives can be obtained readily. The following characteristics, which can be derived with little difficulty, are listed for reference:

$$\left(\frac{\gamma}{C_L}\right)_\alpha = \frac{4}{\pi} \sqrt{1 - (y^*)^2}$$

$$c^* = \frac{8}{\pi A} \sqrt{1 - (y^*)^2}$$

$$\tan \Lambda = \frac{2}{\pi A} \frac{y^*}{\sqrt{1 - (y^*)^2}}$$

$$\frac{d\left(\frac{\gamma}{C_L}\right)_\alpha}{dy^*} = - \frac{4}{\pi} \frac{y^*}{\sqrt{1 - (y^*)^2}}$$

These relationships can be used with equations (A9) and (A15) to obtain

$$\frac{d\gamma}{d\beta} = \frac{32}{\pi^2 A} y^* C_L \quad (A26)$$

and

$$\frac{C_{L_\beta}}{C_L} = - \frac{16}{3\pi^2 A} + 0.05 \quad (A27)$$

Wings with straight leading and trailing edges - integration method.-  
The chord of a wing having straight leading and trailing edges over each semispan is given by

$$c^* = \frac{4}{A(1 + \lambda)} \left[ 1 - (1 - \lambda)y^* \right] \quad (A28)$$

Equation (A28) can be used with equations (A9) and (A17) to obtain

$$\frac{d\gamma}{d\beta} = (\gamma)_\alpha \tan \Lambda - \frac{3}{A(1 + \lambda)} \left[ 1 - (1 - \lambda)y^* \right] \frac{d(\gamma)_\alpha}{dy^*} \quad (A29)$$

and

$$\frac{c_{l\beta}}{c_L} = -\frac{1}{2} \left\{ \frac{3}{A(1+\lambda)} + \bar{y}^* \left[ \tan \Lambda - \frac{6(1-\lambda)}{A(1+\lambda)} \right] \right\} + 0.05 \quad (A30)$$

Elliptic wing - step-load method.- The following characteristics of elliptic wings, when represented by horseshoe vortices, can be readily derived and are listed for reference. For the right semispan,

$$\left[ \left( \frac{\gamma}{c_L} \right)_{\alpha} \right]_n = \frac{4}{\pi N} \sqrt{N^2 - (2n-1)^2}$$

$$(c_o^*)_n = \frac{8}{\pi NA} \sqrt{N^2 - 4n^2}$$

$$(c_i^*)_n = \frac{8}{\pi NA} \sqrt{N^2 - 4(n-1)^2}$$

$$(\tan \Lambda)_n = \frac{1}{\pi A} \left[ \sqrt{N^2 - 4(n-1)^2} - \sqrt{N^2 - 4n^2} \right]$$

These relationships can be used with equation (A25) to obtain

$$\frac{c_{l\beta}}{c_L} = -\frac{4}{\pi^2 AN^3} \left\{ \sum_{n=1}^{n=N/2} \left[ (4n+1) \sqrt{N^2 - 4n^2} - (4n-5) \sqrt{N^2 - 4(n-1)^2} \right] \sqrt{N^2 - (2n-1)^2} \right\} + 0.05 \quad (A31)$$

Wings with straight leading and trailing edges - step-load method.- The local chord of a wing having straight leading and trailing edges over each semispan is given by equation (A28). The chords can also be expressed as

$$(c_o^*)_n = \frac{4}{A(1+\lambda)} \left[ 1 - (1-\lambda) \frac{2n}{N} \right]$$

and

$$(c_i^*)_n = \frac{4}{A(1+\lambda)} \left[ 1 - (1-\lambda) \frac{2n-2}{N} \right]$$



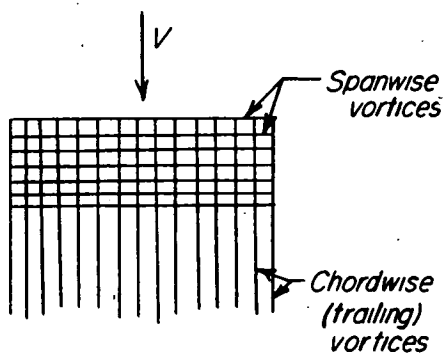
These expressions can be used with equation (A25) to obtain

$$\frac{C_{L_B}}{C_L} = \frac{3}{A(1 + \lambda)N^2} \left\{ \sum_{n=1}^{n=N/2} \left[ (4n - 2)(1 - \lambda) - N - \frac{(2n - 1)(1 + \lambda)}{3} A \tan \Lambda \right] \left[ \left( \frac{\gamma}{C_L} \right)_{\alpha} \right]_n \right\} + 0.05 \quad (A32)$$

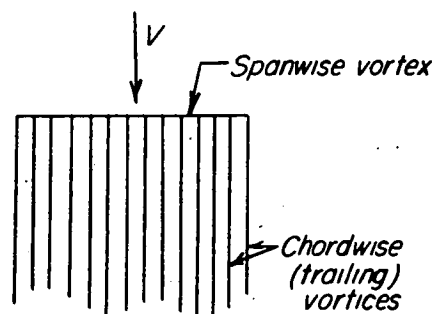
## REFERENCES

1. Weissinger, J.: Der schiebende Tragflügel bei gesunder Strömung. Bericht S 2 der Lilenthal-Gesellschaft für Luftfahrtforschung, 1938-39, pp. 13-51.
2. Luckert, H. J.: Lift Distribution on Swept-Back Wings in Yaw. Reps. and Translations No. 741 (AGD Rep. No. 1066), British M.O.S. (A) Völkenrode, Mar. 1947.
3. Jacobs, W.: Systematische Druckverteilungsmessungen an Pfeilflügeln konstanter Tiefe bei symmetrischer und unsymmetrischer Anströmung. Bericht 44/28, Aerodynamisches Institut der T. H. Braunschweig, Nov. 8, 1944.
4. DeYoung, John, and Harper, Charles W.: Theoretical Symmetric Span Loading at Subsonic Speeds for Wings Having Arbitrary Plan Form. NACA Rep. 921, 1948.
5. Diederich, Franklin W., and Zlotnick, Martin: Calculated Spanwise Lift Distributions and Aerodynamic Influence Coefficients for Unswept Wings in Subsonic Flow. NACA TN 3014, 1953.
6. Diederich, Franklin W., and Zlotnick, Martin: Calculated Spanwise Lift Distributions and Aerodynamic Influence Coefficients for Swept Wings in Subsonic Flow. NACA TN 3476, 1955.
7. Diederich, Franklin W., and Latham, W. Owen: Calculated Aerodynamic Loadings of M, W, and A Wings in Incompressible Flow. NACA RM L51E29, 1951.
8. Blenk, Hermann: The Monoplane as a Lifting Vortex Surface. NACA TM 1111, 1947.
9. Campbell, George S.: A Finite-Step Method For the Calculation of Span Loadings of Unusual Plan Forms. NACA RM L50L13, 1951.
10. Gray, W. L., and Schenk, K. M.: A Method for Calculating the Subsonic Steady-State Loading on an Airplane With a Wing of Arbitrary Plan Form and Stiffness. NACA TN 3030, 1953.
11. Toll, Thomas A., and Queijo, M. J.: Approximate Relations and Charts for Low-Speed Stability Derivatives of Swept Wings. NACA TN 1581, 1948.
12. Goodman, Alex, and Brewer, Jack D.: Investigation at Low Speeds of the Effect of Aspect Ratio and Sweep on Static and Yawing Stability Derivatives of Untapered Wings. NACA TN 1669, 1948.

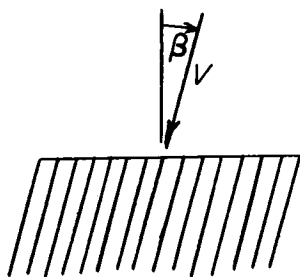
13. Jaquet, Byron M., and Brewer, Jack D.: Low-Speed Static-Stability and Rolling Characteristics of Low-Aspect-Ratio Wings of Triangular and Modified Triangular Plan Forms. NACA RM L8L29, 1949.
14. Goodman, Alex, and Thomas, David F., Jr.: Effects of Wing Position and Fuselage Size on the Low-Speed Static and Rolling Stability Characteristics of a Delta-Wing Model. NACA TN 3063, 1954.
15. Letko, William, and Cowan, John W.: Effect of Taper Ratio on Low-Speed Static and Yawing Stability Derivatives of  $45^\circ$  Sweptback Wings With Aspect Ratio of 2.61. NACA TN 1671, 1948.
16. Jaquet, Byron M.: Effect of Linear Spanwise Variations of Twist and Circular-Arc Camber on Low-Speed Static Stability, Rolling, and Yawing Characteristics of a  $45^\circ$  Sweptback Wing of Aspect Ratio 4 and Taper Ratio 0.6. NACA TN 2775, 1952.



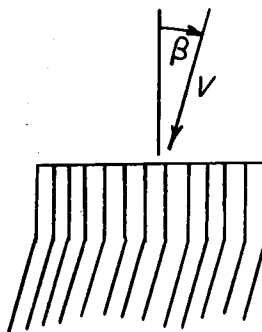
(a) General arrangement for zero sideslip.



(b) Lifting-line-theory arrangement for zero sideslip.

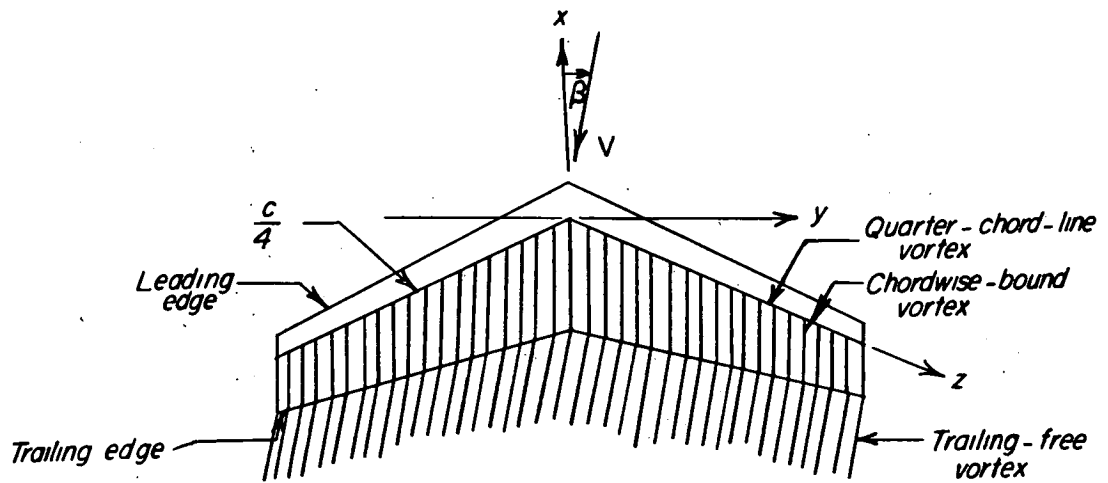


(c) Blenk's arrangement (ref. 8) for sideslip.

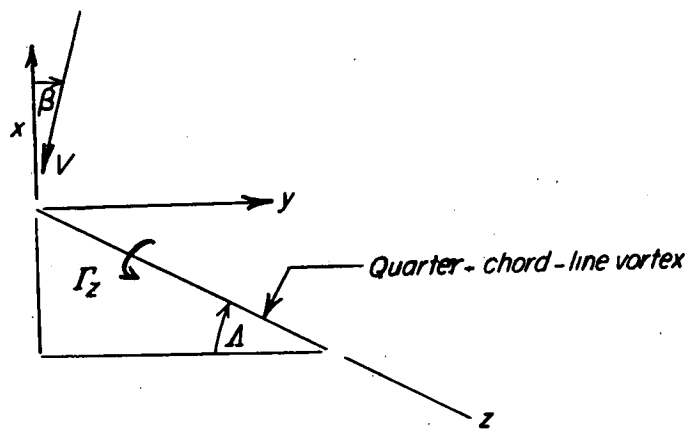


(d) Weissinger's arrangement (ref. 1) for sideslip.

Figure 1.—Vortex systems used for representing unswept wings.

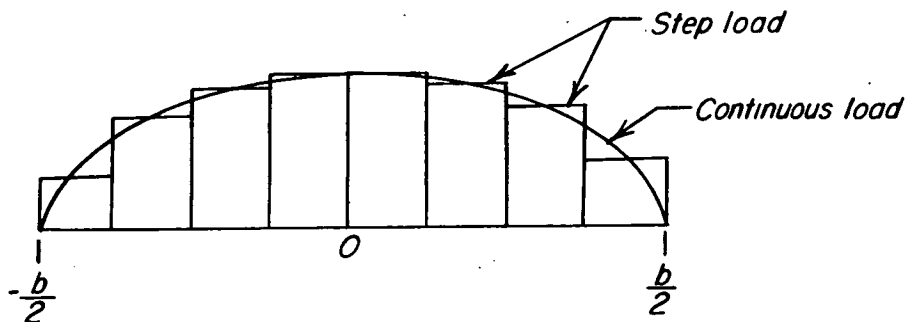


(a) Overall representation.

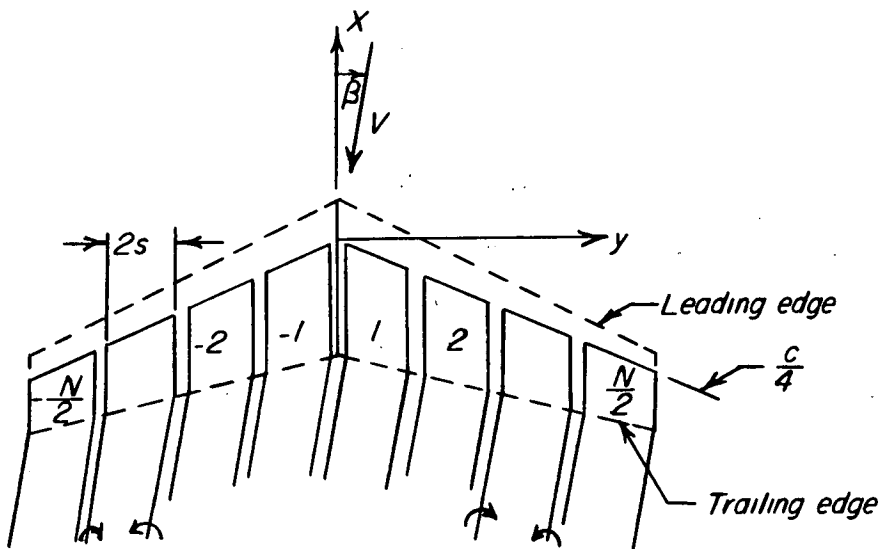


(b) Details of an element of the quarter-chord-line vortex.

Figure 2.— Representation of a wing by the vortex system used in analysis.



(a) Approximation of continuous load by step load.



(b) Representation of a wing by a finite number of horseshoe vortices.

Figure 3.— Representation of wing when span load is assumed to be made up of spanwise step loadings.

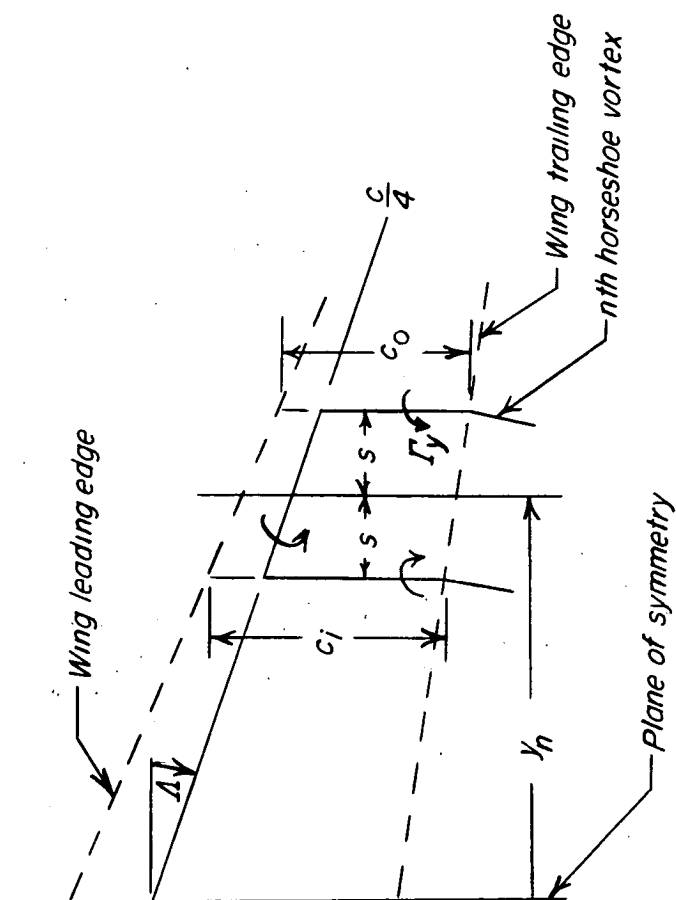


Figure 4.- Details of  $n$ th horseshoe vortex used in representing wing in sideslip by a number of horseshoe vortices.

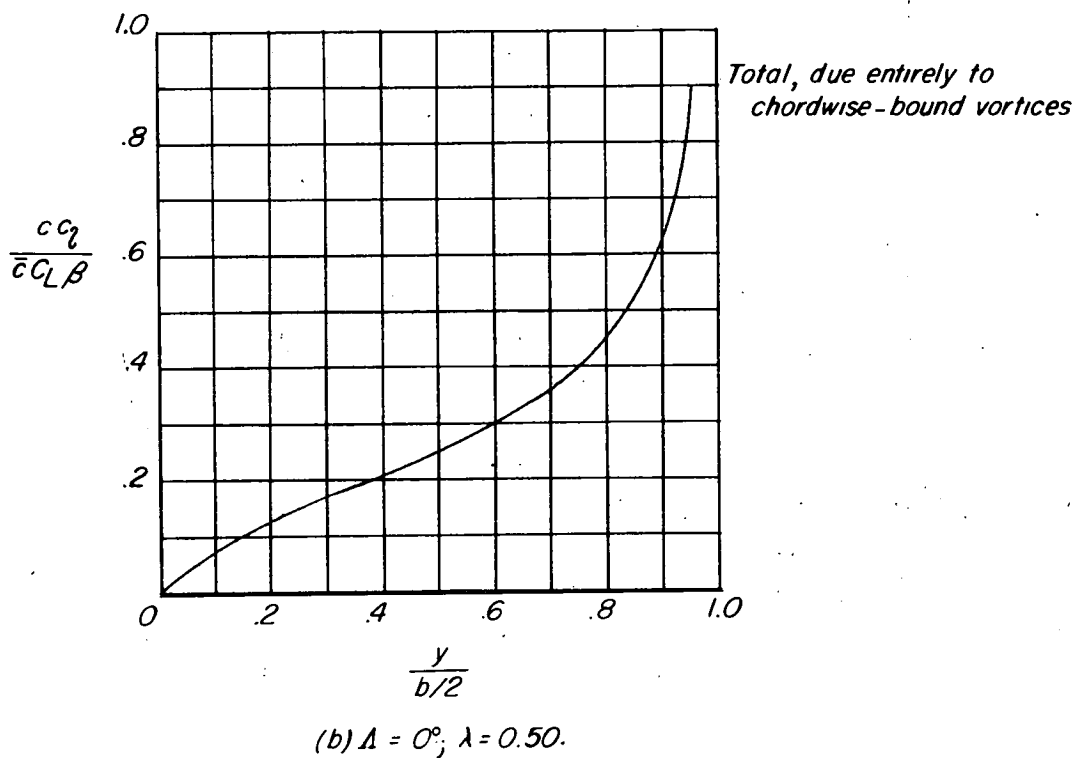
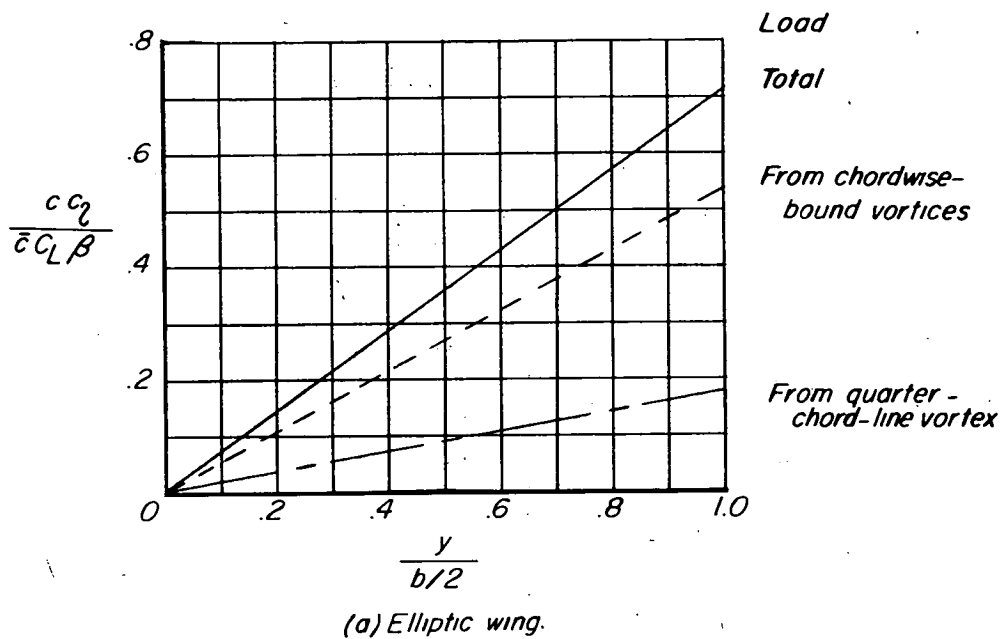
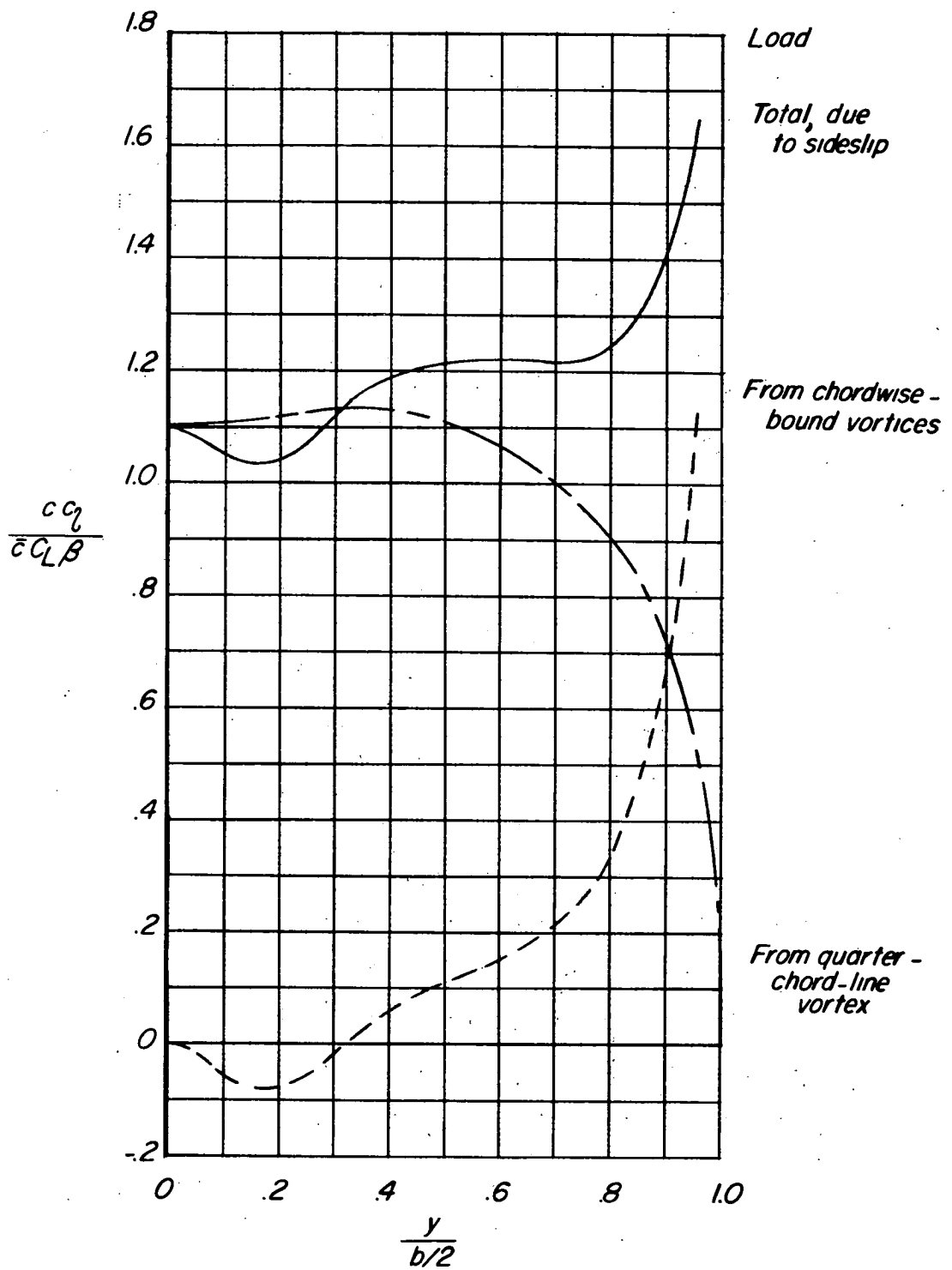


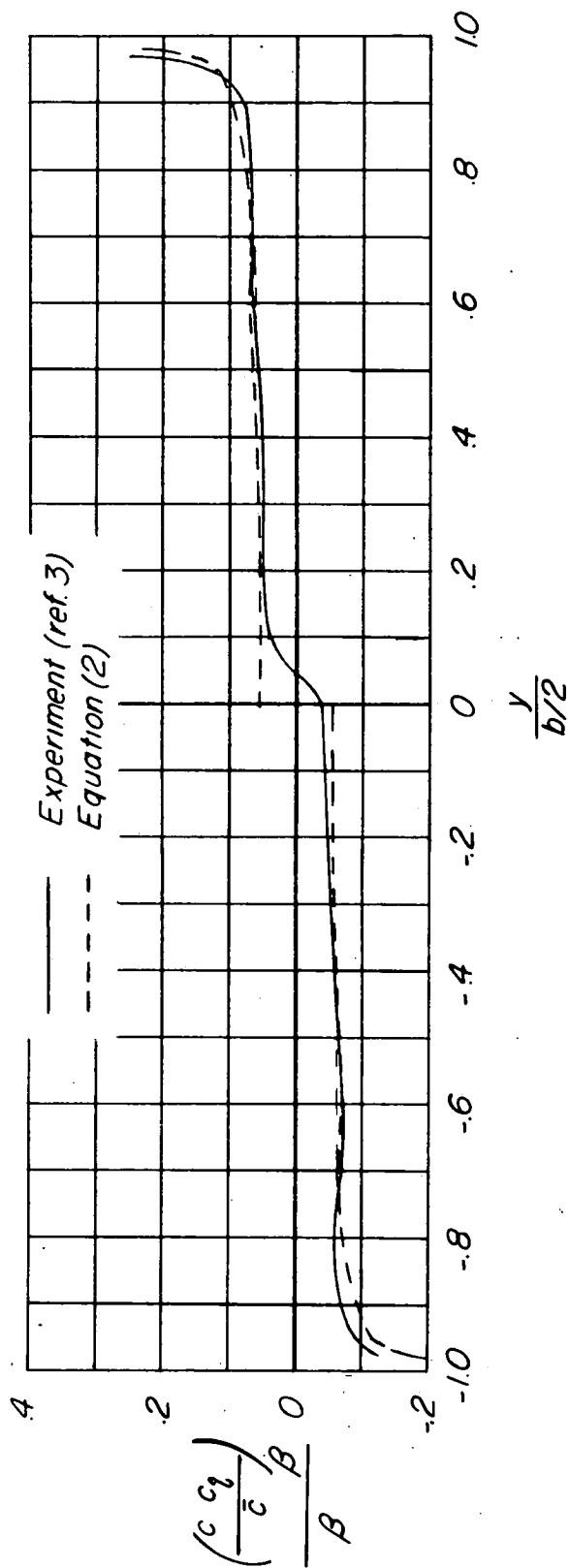
Figure 5.- Estimated span load due to sideslip for several plane wings.  $A = 4.5$ .





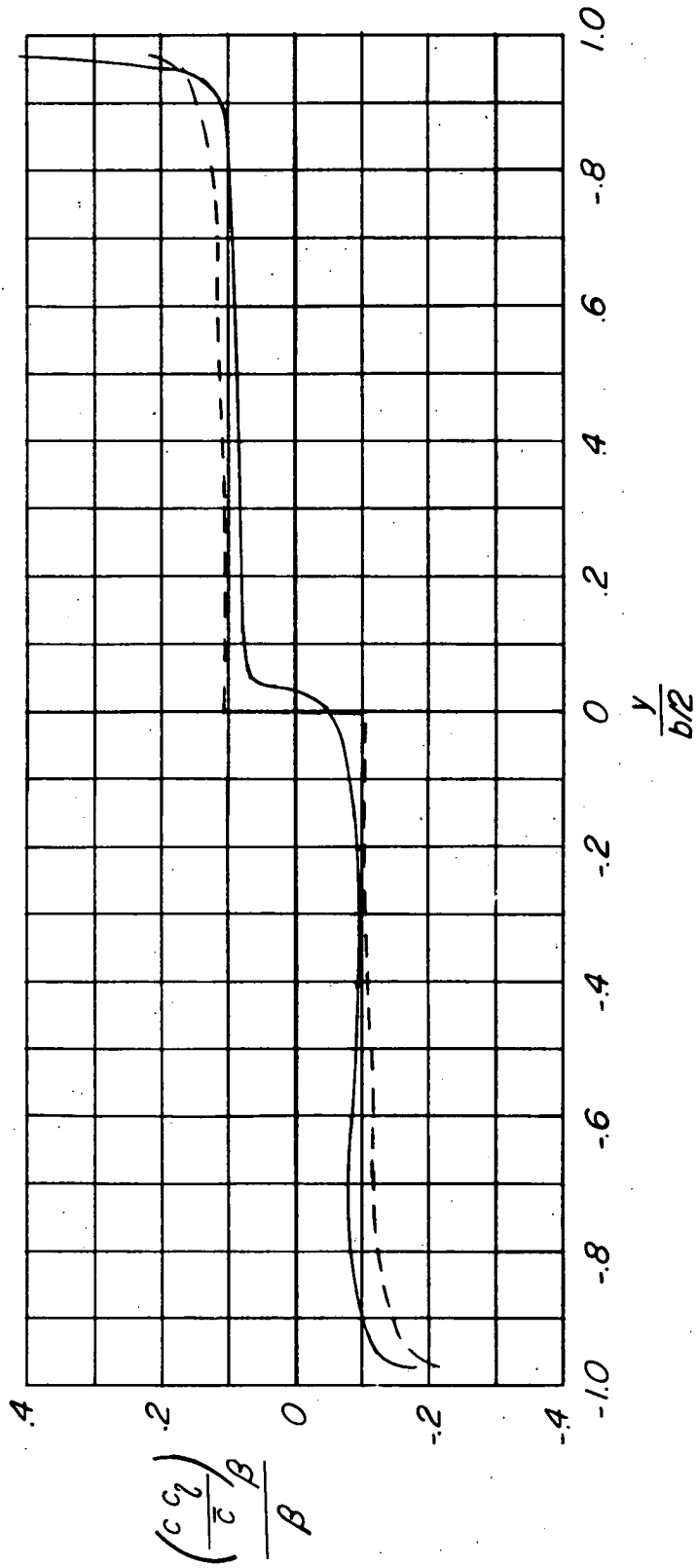
(c)  $\Delta = 45^\circ$ ;  $\lambda = 0.50$ .

Figure 5.- Concluded.



(a)  $A=5.16$ ;  $\Lambda=45^\circ$ ;  $\lambda=1.00$ ;  $\alpha=5.7^\circ$ ; and  $\beta=10^\circ$

Figure 6.- Comparison of experimental and calculated span loads due to sideslip



(b)  $A = 5.16$ ;  $\Delta = 45^\circ$ ;  $\lambda = 1.00$ ;  $\alpha = 11.5^\circ$ ; and  $\beta = 10^\circ$

Figure 6.- Concluded.

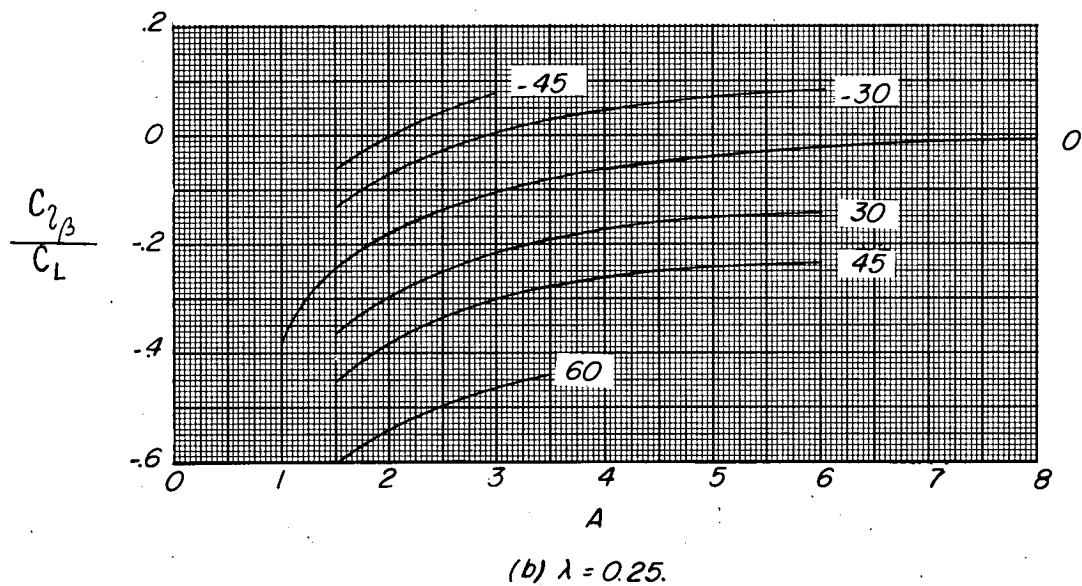
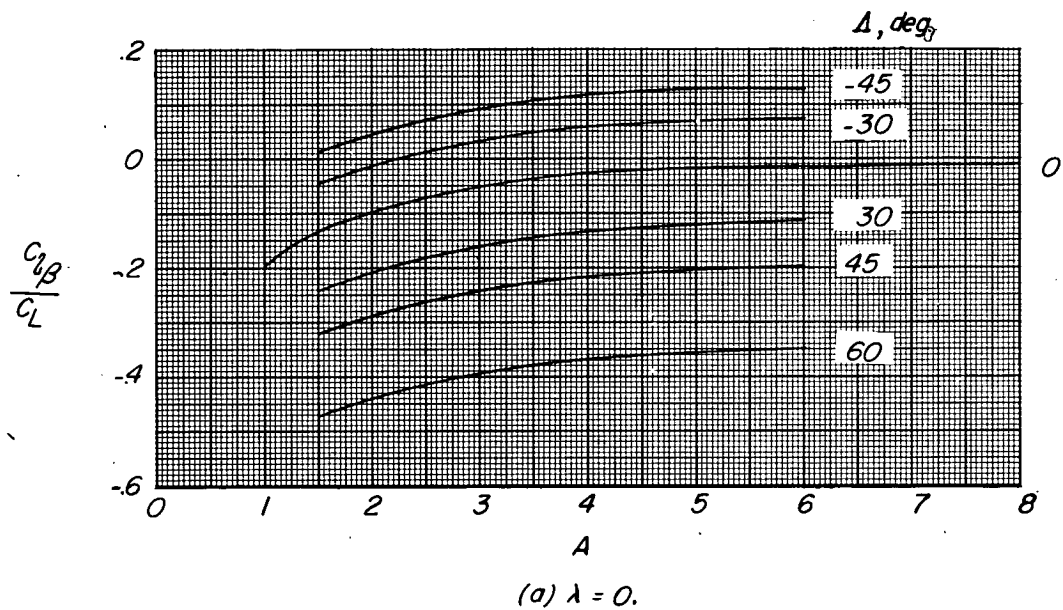


Figure 7.- Variation of  $\frac{c_{l\beta}}{c_L}$  with aspect ratio, taper ratio, and sweep.

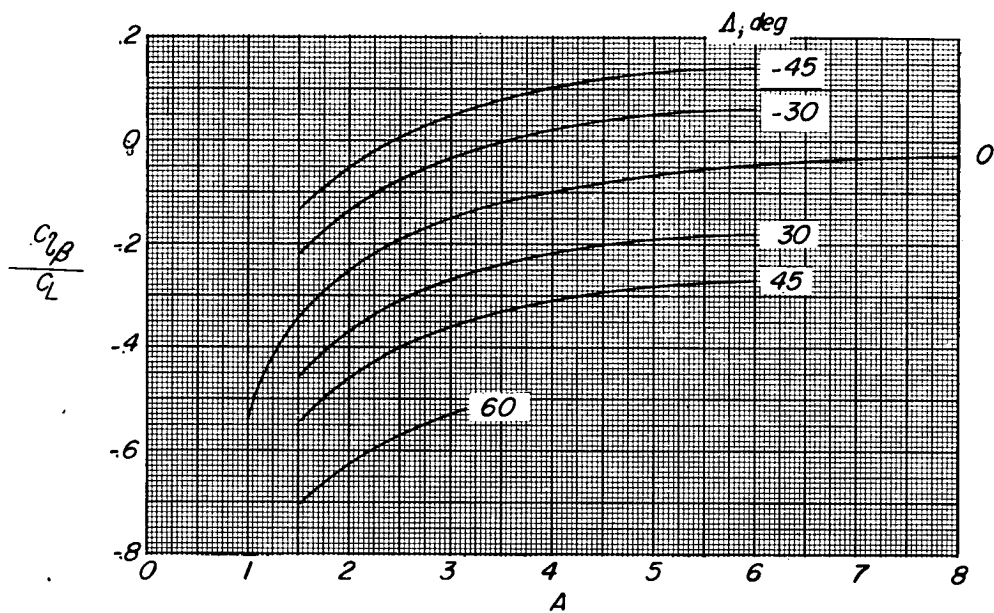
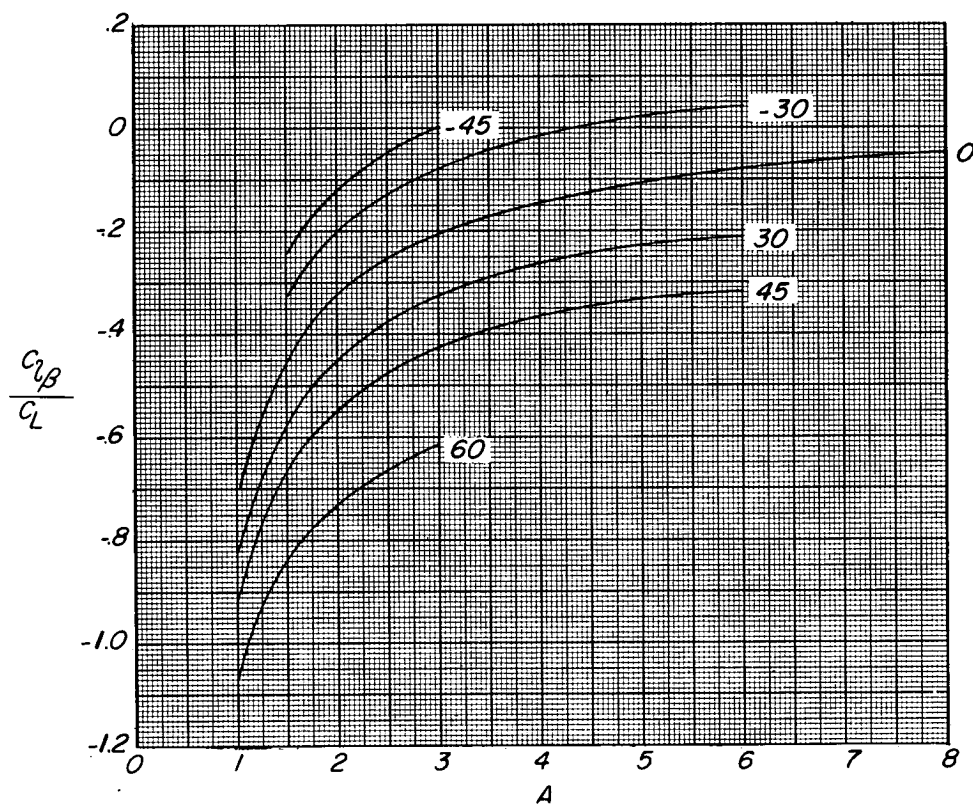
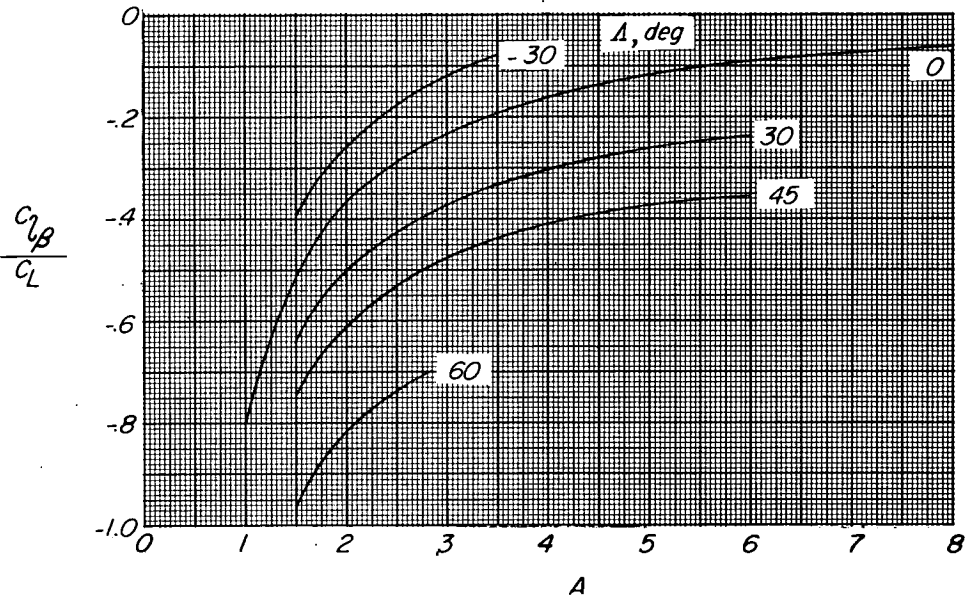
(c)  $\lambda = 0.50$ .(d)  $\lambda = 1.00$ .

Figure 7- Continued.



(e)  $\lambda = 1.50$ .  
Figure 7.- Concluded

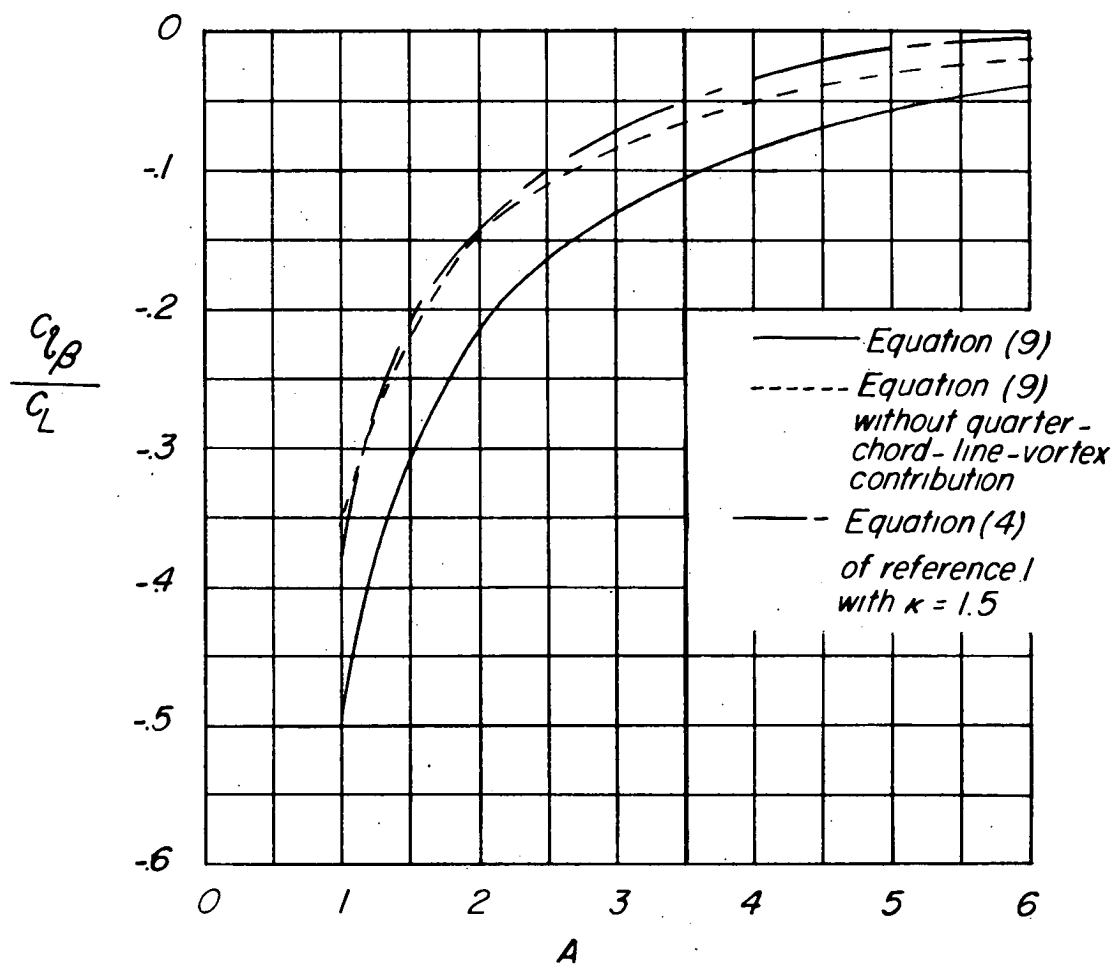


Figure 8.- Coefficient of rolling moment due to sideslip for elliptic wings.

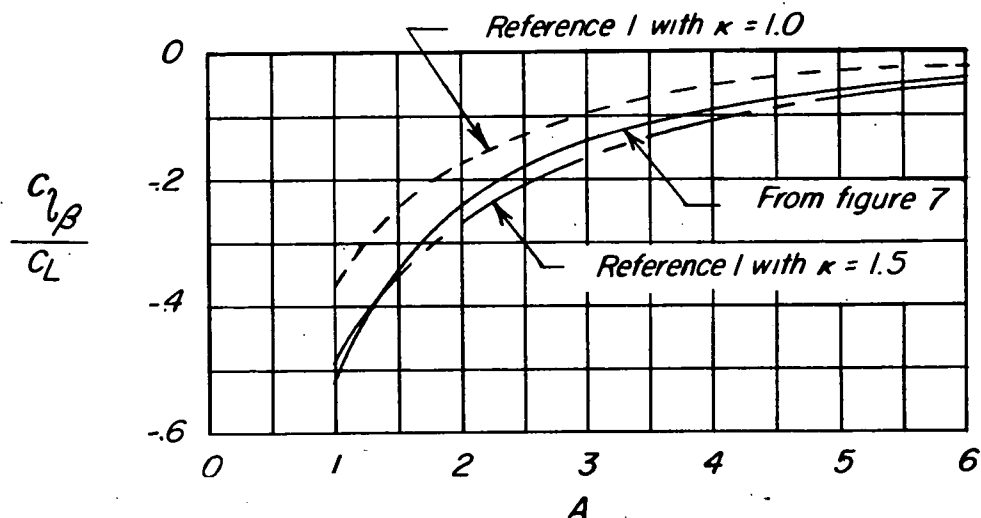
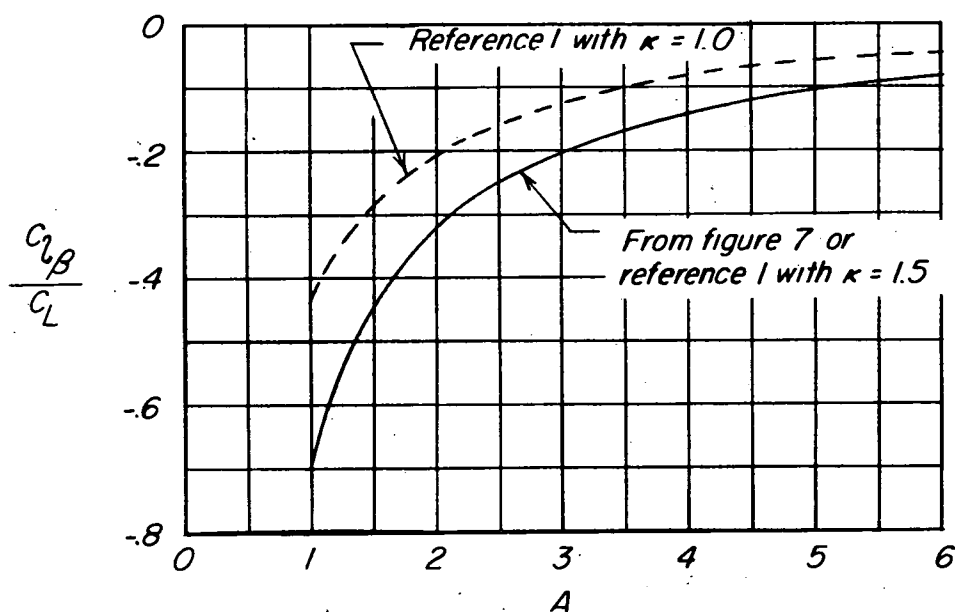
(a)  $\lambda = 0.50$ .(b)  $\lambda = 1.00$ .

Figure 9.- Comparison of values of  $\frac{c_{l\beta}}{c_L}$  from figure 7 with theoretical values from reference I.  $\Lambda = 0^\circ$



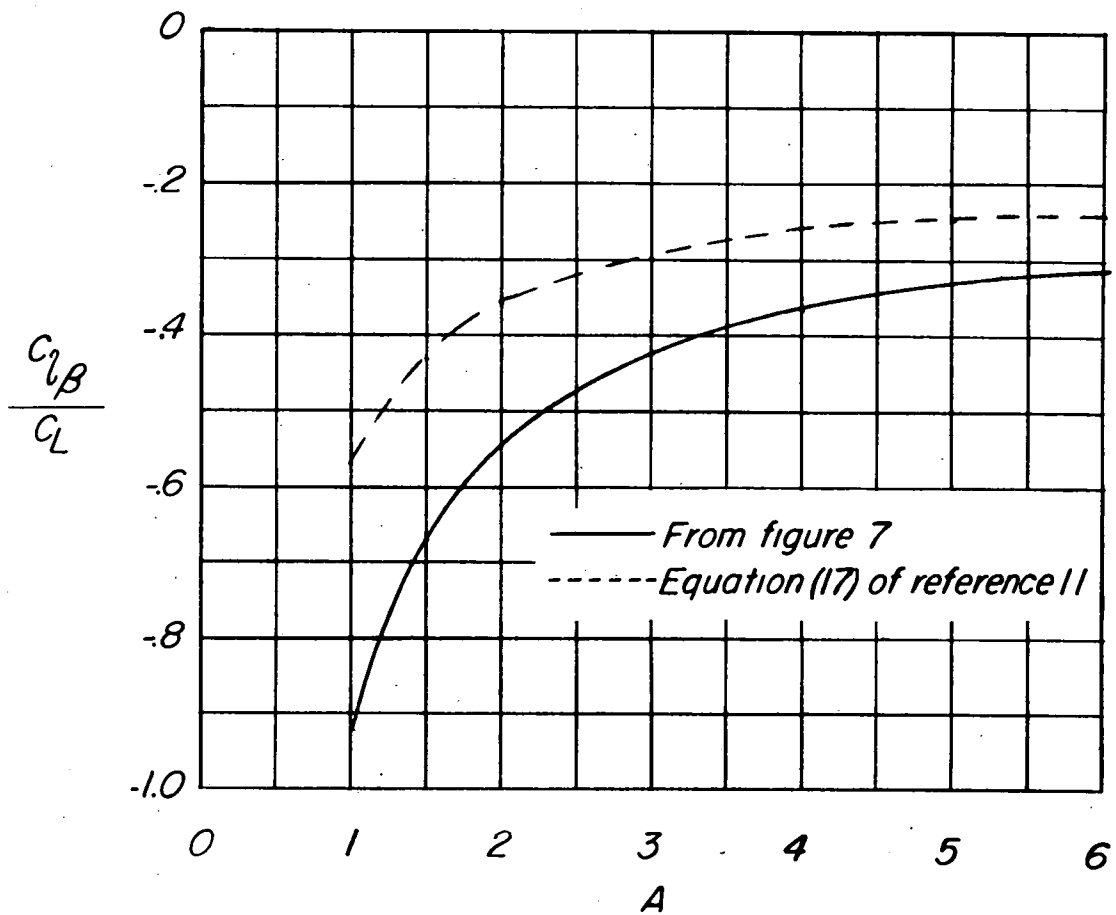
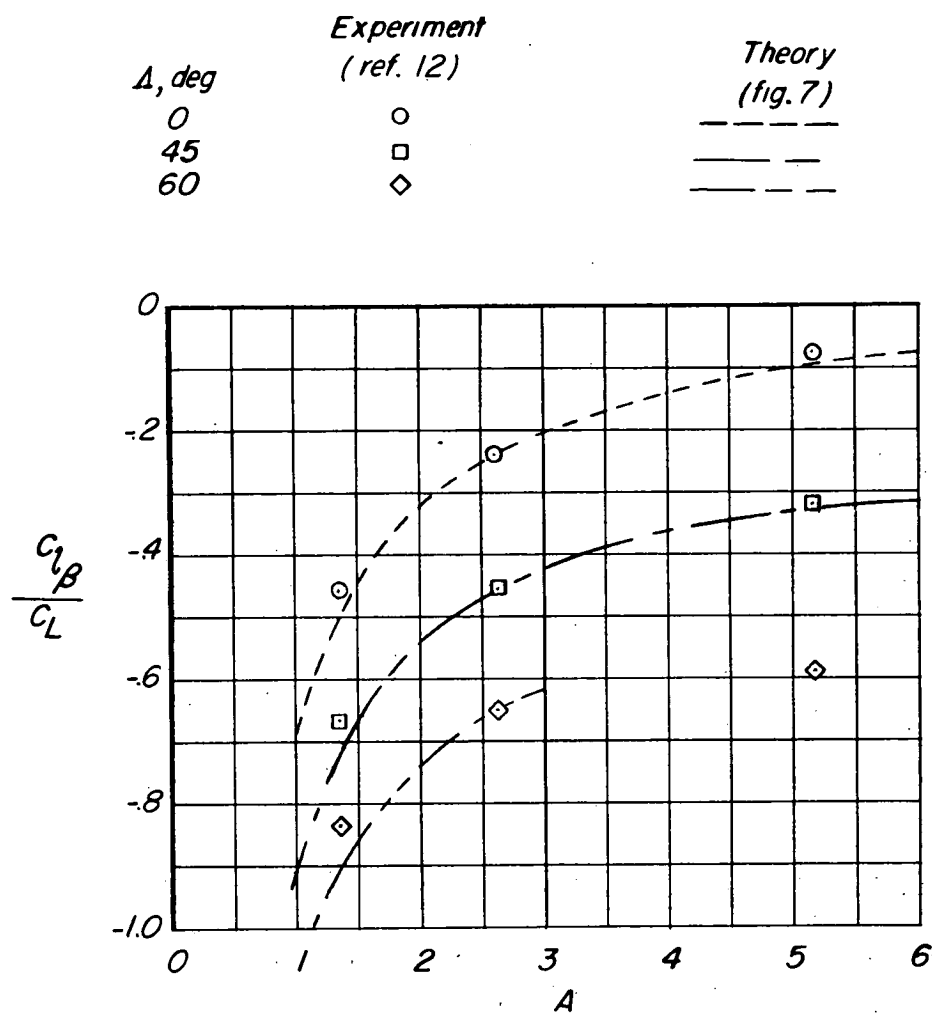
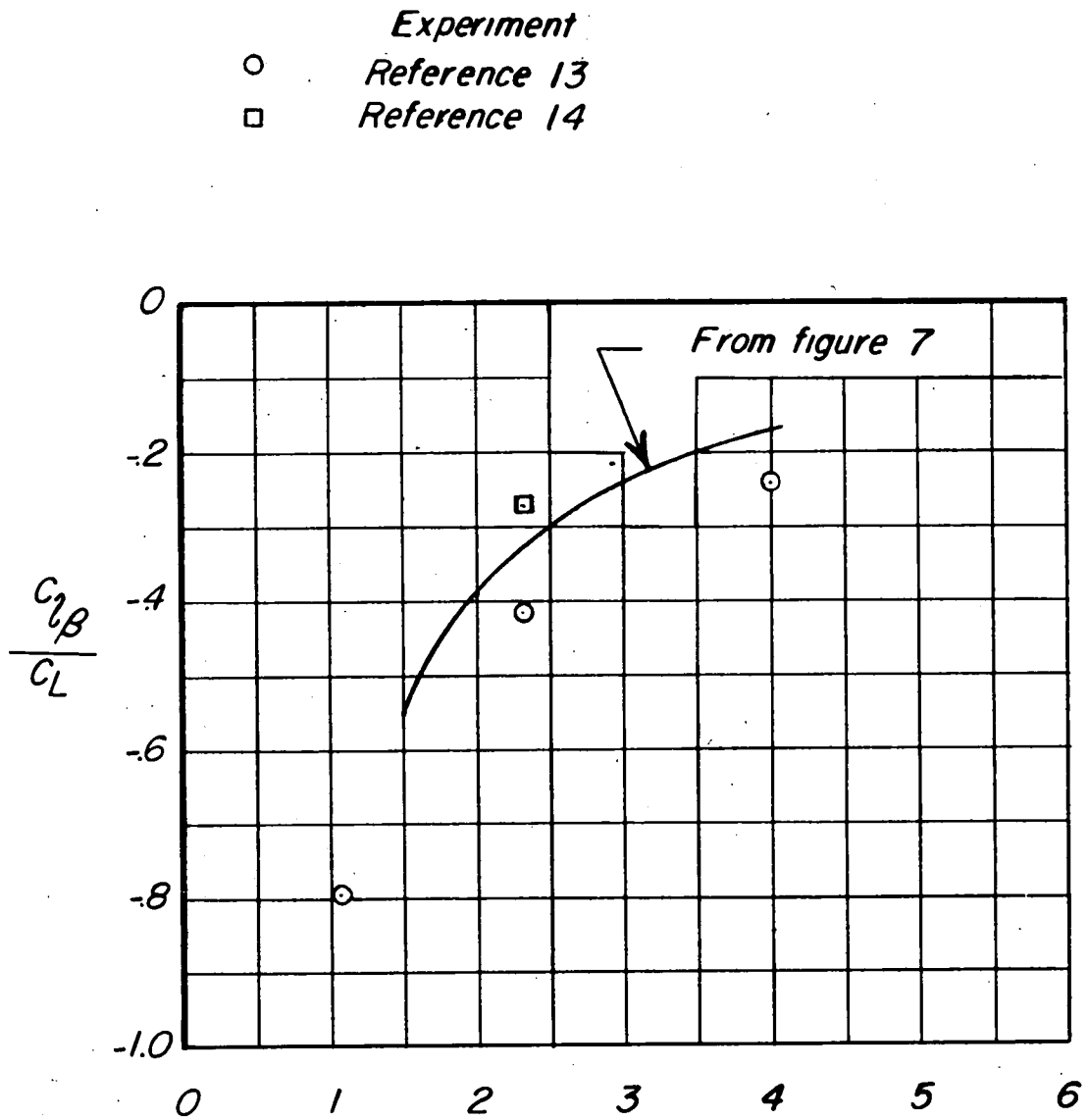


Figure 10.- Comparison of values of  $\frac{C_{l\beta}}{C_L}$  from figure 7 with theoretical values from reference 11.  $\Lambda = 45^\circ$ ;  $\lambda = 1.00$ .



(a) Untapered wings.

Figure 11.- Comparison of experimental and calculated low-speed values of  $\frac{C_{l\beta}}{C_L}$ .



(b) *Triangular wings.*  
*Figure 11.- Concluded.*

Experiment  
 ○ Reference 15

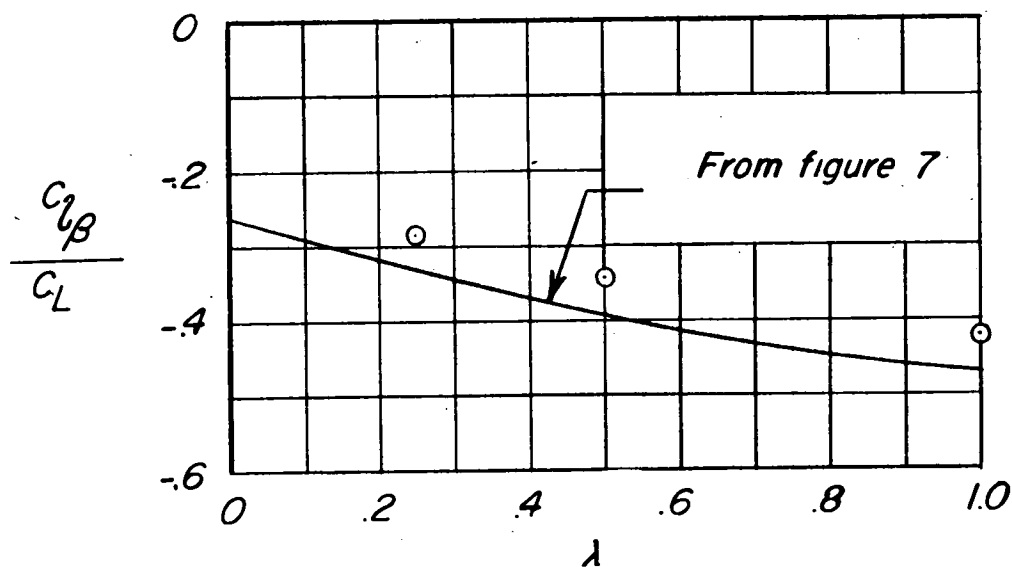
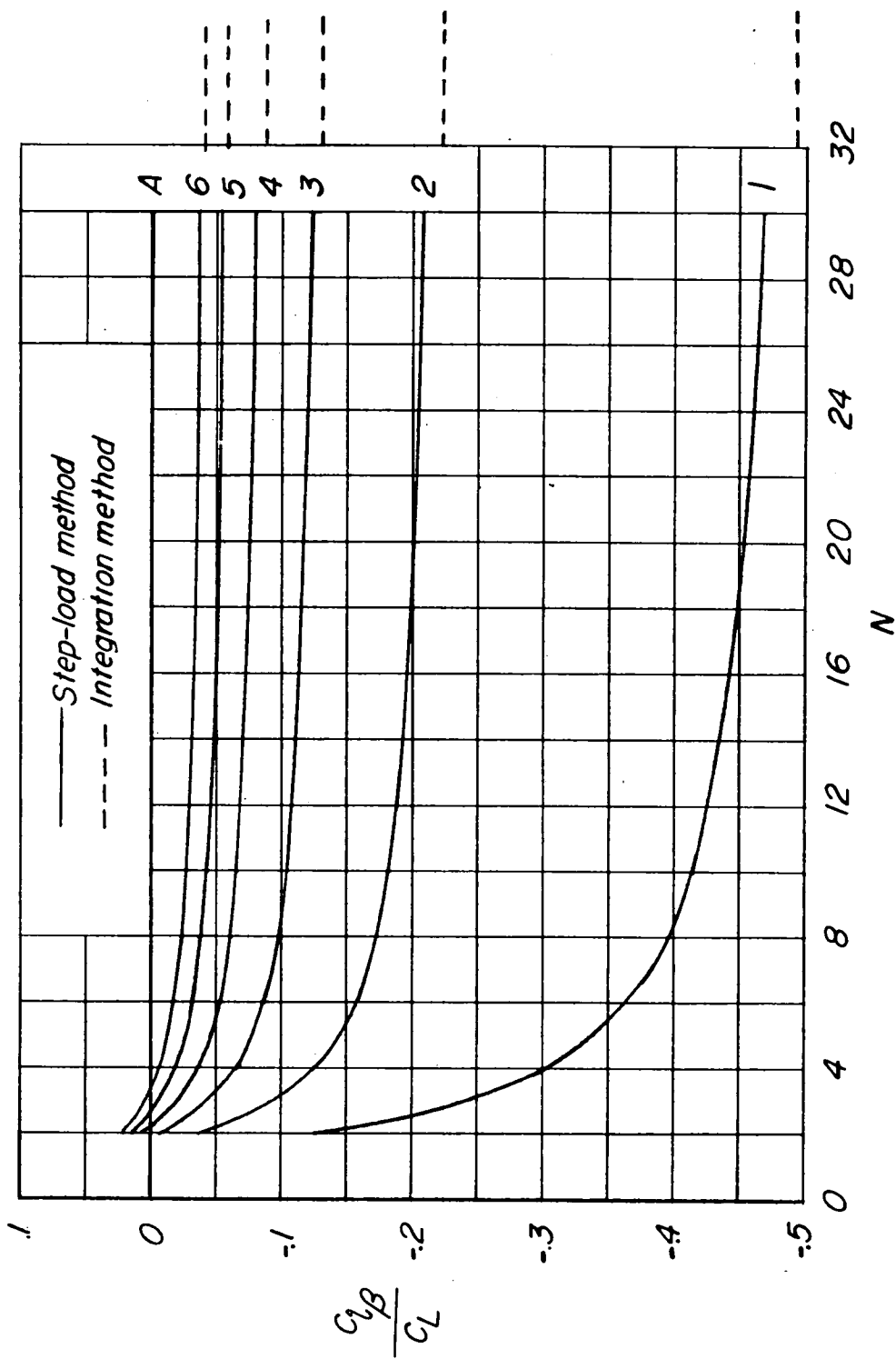


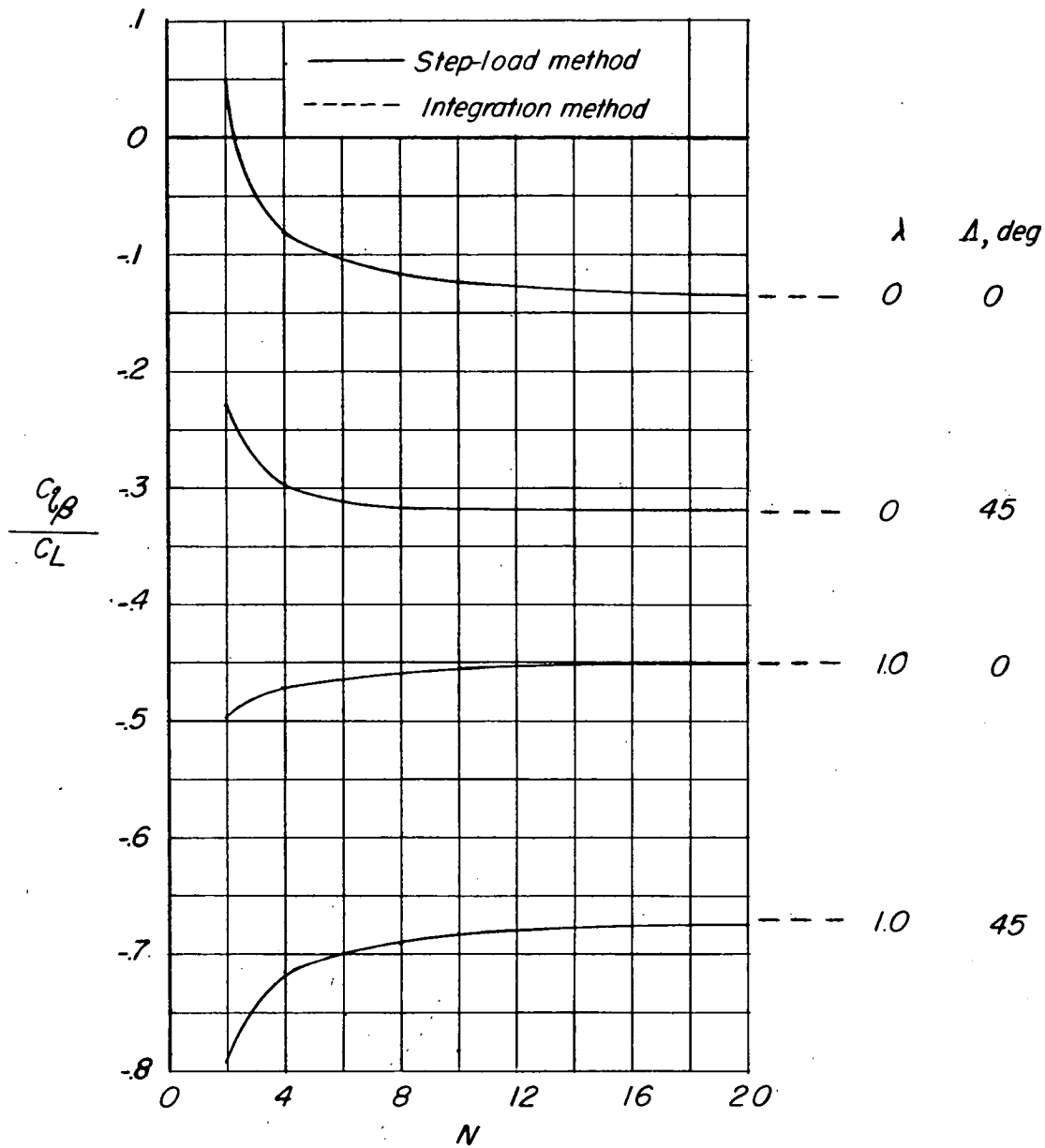
Figure 12.- Comparison of experimental and calculated effect

of  $\lambda$  on  $\frac{c_{l\beta}}{c_L}$ .  $A = 2.61$ ;  $\Lambda = 45^\circ$ .



(a) Elliptic wings.

Figure 13.- Effect of  $N$  on estimated value of  $c_{l\beta}/c_L$ .



(b) Tapered wings,  $A = 1.5$ .  
Figure 13.- Concluded.